



University of Leoben
Chair of Petroleum and Geothermal Energy Recovery
Univ.-Prof. Dipl.-Ing. Dr. mont. Herbert Hofstätter



Designing a Borehole Simulator for Ultrasonic Treatments

Master Thesis
of

Bernd Karl Strommer

November 2013 – April 2014

Advisors at University: Univ.-Prof. Dipl.-Ing. Dr. mont. Herbert Hofstätter
Sepp Steinlechner, MBA
Dipl.-Ing. Hartwig Kunanz

Statutory Declaration

Affidavit

I hereby declare that the content of this work is my own composition and has not been submitted previously for any higher degree. All extracts have been distinguished using quoted references and all information sources have been acknowledged.

Leoben, _____

Date

Signature

Eidesstattliche Erklärung

Ich erkläre an Eides statt, dass ich die vorliegende Diplomarbeit selbständig und ohne fremde Hilfe verfasst, andere als die angegebenen Quellen und Hilfsmittel nicht benutzt und die den benutzten Quellen wörtlich und inhaltlich entnommenen Stellen als solche erkenntlich gemacht habe.

Leoben, am _____

Datum

Unterschrift

Kurzfassung

Durch den stetigen Rückgang von Erschließungen neuer konventioneller Lagerstätten wurde in den vergangenen Jahren die Forschung an unkonventionellen Lagerstätten bzw. dem Maximieren der Ausbeute bereits vorhandener oder verschlossener Lagerstätten stetig vorangetrieben. Letzteres wird mittels Bohrlochbehandlungen durchgeführt, die in den letzten Jahren sehr an Wichtigkeit gewonnen haben und die Thematik dieser Masterarbeit sind. Diese Behandlungen haben das Ziel die Fließraten von Bohrungen, die durch Paraffine, Asphaltene oder Kalkablagerungen verschmutzt sind, zu verbessern. Behandlungen mit Lösungsmitteln oder Säuren sind die gängigsten Methoden die jedoch negative Begleiterscheinungen mit sich bringen. Diese können die Eigenschaften des Rohöls stark beeinflussen und müssen, im Fall von Säuren, auch nachträglich neutralisiert werden. Neben diesen chemischen Behandlungen besteht auch die Möglichkeit der Reinigung mittels Ultraschalls. Dabei wird eine Ultraschalllanze in das Bohrloch eingeführt die Ultraschallwellen freisetzt und dabei die Fließrate merklich verbessern kann. Zur Untersuchung und Verbesserung dieses Prozesses plant die Firma Progress Ultrasonic AG in Zusammenarbeit mit dem Institut für Petroleum and Geothermal Energy Recovery einen Simulator zu bauen, um bohrloch-nahe Bedingungen im Labor zu rekonstruieren. Der Simulator soll Aufschluss über die Reinigungsmechanismen der Ultraschallbehandlung geben und zusätzlich beim Design der sogenannten "Sonotrode" unterstützen und zur Qualitäts- und Beweissicherung dienen.

Für dieses Vorhaben wurden zwei Rohentwürfe erstellt, wovon der erste den ursprünglichen Kriterien entsprach, die sich jedoch im Laufe der Entwicklung verändert haben. Dieser Entwurf sah vor, 3 verschiedenen Komplettierungen drucklos zu testen. Hauptaugenmerk sollte dabei auf die Messung der Abschwächung der Ultraschallwellen durch den, wenn vorhandenen, Zement und der Formation liegen. Die Formation sollte durch einen porösen Zement ersetzt werden, um eine entsprechende Konstruktion zu ermöglichen. Der zweite Entwurf basierte im wesentlichen auf dem ersten bis auf die Tatsache, dass dieser in einem Druckbehälter verbaut werden würde, um unter erhöhtem hydrostatischen Druck zu prüfen.

Labormessungen mit einem Ultraschallgerät durchgeführt zeigten, dass die Ultraschallwellen nur durch die Perforationen nach außen dringen, da der Mantel des Casings den größten Teil der Ultraschallwellen abfängt. Außerdem zeigten bereits durchgeführte Ultraschalltests zur Brunnenreinigung unter hydrostatischen Drücken von bis zu 20 bar, dass Kavitation ab Drücken von 5 bar vernachlässigbar klein wird. Aus diesem Grund änderte sich der finale Entwurf dahingehend, dass das Hauptaugenmerk der Tests auf der Untersuchung der tatsächlich auftretenden Reinigungsmechanismen unter hohem hydrostatischen Druck und hoher Temperatur liegt. Dazu wurde ein Druckbehälter geplant, indem die Ultraschallsonde entweder mit oder ohne Casing in verschiedenen Flüssigkeiten getestet werden kann.

Abstract

Due to decreasing development of new conventional reservoirs the research in new unconventional sources and the increase in recovery of existing or already abandoned wells has become an important target for the future. The latter is done with different well treatments, where acidizing and flushing with solvent are the standard procedures to improve the flow behavior of plugged or polluted wells. Thereby the pollution originates from associated substance in the crude oil which form in many cases precipitations, asphaltenes, scale and paraffins. However, the treatments with acids and solvents show several negative concomitant effects like degradation of crude oil or the need of neutralization which introduced the search for alternative treatment methods. One of them are well treatments with ultrasonic waves which is the topic of this master thesis.

Ultrasonic treatments are performed by inserting an ultrasonic resonator into the well and producing ultrasonic waves for a certain time. This can lead to considerably improvements in flow rate. Nevertheless, the process of cleaning is very complex and even at elevated hydrostatic pressure and temperature not a well known topic. Therefore the company Progress Ultrasonic AG in cooperation with the chair of Petroleum and Geothermal Energy Recovery want to build a simulator for the laboratory, to test the behavior of ultrasonic treatments on well, perforations and the near wellbore area. Furthermore, the design of the "sonotrode" and the quality management should be improved.

For this purpose two drafts have been made. The first one fitted the initial requirements, but those changed during the hole development process. Testing the attenuation through three completions under hydrostatic pressure, elevated temperature and saturated in different fluids were the main focus of the first draft. The second one offered additionally the possibility to test above atmospheric pressure.

Laboratory tests in a water bath with the ultrasonic resonator at atmospheric pressure showed that casing shields the formation from the ultrasonic waves and nearly no waves traveled through it except for the perforations. Additional tests for aquifer cleaning from the university of Mainz indicated, that the effects of cleaning change with increasing hydrostatic pressure. Cavitation, which is responsible for cleaning at atmospheric pressure, becomes negligible small above 5 *bar* hydrostatic pressure. Out of that a final simulator was designed, focusing on the study of the cleaning processes at elevated pressures and temperatures. In this simulator the ultrasonic device can be tested in different fluids with or without a casing. It is a sealed cylindrical pipe where the fluid can be pumped into it via a connection at the bottom. Since there will be test runs with borehole fluids, the simulator is standing in a box, to avoid a spill in in case of a leakage.

Acknowledgement

I would like to express my gratitude to my supervisor Univ.-Prof. Dipl.-Ing. Dr. mont. Herbert Hofstätter and the company Progress Ultrasonic AG that shared their precious time to give me the opportunity to write a thesis about this interesting topic. I am also grateful to Dipl.-Ing. Hartwig Kunanz for his useful remarks, comments and engagement through the process of this master thesis. Furthermore, I like to thank Sepp Steinlechner, MBA for spending his time to read this thesis as well for the support on the way and providing useful suggestions.

Last but not less important, I want to thank my family for their financial support and encouragement throughout my whole life. Without their love and patience, none of this would have been possible.

List of Figures

1	Open hole completion and screen completion [2]	4
2	Cemented/perforated casing and pre-slotted liner [4]	4
3	Production well damage due to scale [5, p. 35]	6
4	Scematic figure of paraffin deposition [7, p. 37]	7
5	Wax appearance temperature (WAT) [9]	7
6	Asphaltene Precipitation Envelope [10]	8
7	Casing scraper [13, p. 44] and pigs [14, p. 1] for removing precipitations	10
8	Propagation of a longitudinal wave through gases and liquids [18]	12
9	Propagation of the shear wave [19]	13
10	Diffraction and refraction of the incoming primary wave between two fluids or gases	14
11	Dipole moment induced by mechanical deformation of quartz crystal [20]	15
12	Chain structure of a PVDF crystal [23]	17
13	Charge distribution inside the film after treatment with the electric field [21, p. 346]	18
14	Sinus shaped wave which is steepening [21, p. 83]	18
15	Gas filled micro gap on a solid surface [17, p. 347]	20
16	Growth of a cavitation bubble [21, p. 91]	21
17	Deformation of the cavitation bubble in presence of a wall or another bubble [17, p. 353]	21
18	Formation of a jet [24]	22
19	Piezoelectric ring with isolated end caps [25, p. 163]	26
20	Tonpitz piston hydrophone with piezoelectric stack [25, p. 169]	27
21	Simplified dual bender piezoelectric disc hydrophone [25, p. 175]	27
22	Operation principle of the DFB fiber laser hydrophone [28, p. 629]	29
23	Exploded view of of the sensor structure [29, p. 5]	30
24	Cross section of the sensor chip with details of the parts [29, p. 6]	31
25	Construction of the ultrasonic wireline tool [17, p. 353]	33
26	Example of a perforated casing completion in the simulator	35
27	A 3D view of the simulator with the the closed hinge	36
28	Details from the hinge and the cable tracks	36
29	Details of the case of the second concept	37
30	Cross-sectional view of the second concept	38
31	Ultrasonic generator	39
32	Ultrasonic resonator	39

33	Test set-up for the ultrasonic treatment	40
34	Ultrasonic treatment in a water bath 50 <i>cm</i> away from the resonator without a casing	41
35	Ultrasonic treatment in a water bath 10 <i>cm</i> away from the resonator	41
36	Test set up for the perforated casing	42
37	Test run with the perforated casing, perforations pointing at the aluminum foil at a distance of 20 <i>cm</i>	43
38	Example of a perforated casing and the casing for the laboratory tests	43
39	Ultrasonic test in a water bath 10 <i>cm</i> away from the resonator with the perforated casing	43
40	Ultrasonic treatment for a water aquifer [31, p.11]	44
41	First simulation set-up of the final simulator with the casing only	45
42	Second simulation set-up with the casing and the boiler	46
43	Data sheet for hydrophone	49
44	Data sheet for recording and analysing unit	50
45	Data sheet for manometer	51
46	Data sheet for safety valve	52
47	Data sheet for pressure sensor	53
48	Data sheet for screw-in temperature sensor	54
49	Data sheet for ball valve	55
50	Data sheet for pump	56
51	Offer for the frame	57

List of Tables

1	Physical parameters of gases and fluids [17, p. 25]	14
2	Price list of the parts of the simulator	47

Contents

1	Introduction	1
2	Theoretical Fundamentals	3
2.1	Downhole Completions	3
2.2	Perforation Impurities	5
2.2.1	Scale	5
2.2.2	Paraffins	6
2.2.3	Asphaltenes	8
2.3	Conventional Removal	9
2.3.1	Scale	9
2.3.2	Asphaltenes	9
2.3.3	Paraffins	9
2.4	Ultrasonic Waves	11
2.4.1	Generation of Ultrasonic Waves	11
2.4.2	Piezoelectric Effect	15
2.4.3	Behavior in Fluids and Gases	18
2.4.4	Attenuation	23
2.5	Hydrophones	25
2.5.1	Principle of Hydrophones	25
2.5.2	Conventional Hydrophones	26
2.5.3	Optical Hydrophones	28
3	Borehole Simulator	32
3.1	General	32
3.2	Ultrasonic Wireline Tool	32
3.3	Simulator Design Concepts	33
3.4	Laboratory Tests	39
3.4.1	Laboratory Test Device	39
3.4.2	Test Runs at the University	40
3.4.3	Tests for Aquifer Cleaning	44
3.5	Final Simulator	45
3.6	Cost Estimation	47
4	Results/Conclusion	48
5	Appendices	49

Definitions

Expression	Meaning	Unit
corprene	polychloroprene-cork composite	
pay zone	reservoir rock in which oil and gas are found in exploitable quantities	
α	absorption coefficient	$[dB/cm/MHz]$
c	sonic velocity	$[m/s]$
c_L	velocity of the longitudinal wave	$[m/s]$
c_T	velocity of the transversal wave	$[m/s]$
C_V	specific heat constant	$[J/mol/K]$
η_d	dynamic viscosity	$[Pa.s]$
κ	adiabatic constant	[]
λ, μ	Laméschen constants	$[N/m^2]$
ν	heat conductivity	$[W/m/K]$
ω	sound frequency	$[Hz]$
P_{i0}	vapor pressure inside a cavitation bubble	$[Pa]$
P_0	hydrostatic pressure	$[Pa]$
ρ_o	density of the media	$[kg/m^3]$
R_0	radius of the bubble	$[m]$
R_{min}	minimum radius of the bubble	$[m]$
t	time	$[s]$
T_0	room temperature	$[K]$
v	particle velocity	$[m/s]$
ξ, η, ζ	components of the displacement vector	[]
Z	characteristic impedance	$[Ns/m^3]$

1 Introduction

The improvement in the stimulation of production wells has become an important and necessary issue in the petroleum industry. Due to the shrinking development of conventional hydrocarbon reservoirs, enhancing the production life of existing fields is a key target for the future. Even as the reservoir depletes under production, temperature and pressure conditions are changing and form, in many cases, precipitation. These develop from associated substances in the crude oil and are called paraffins and asphaltenes. Moreover, scale forms from the water in the formation that flows along with the hydrocarbons. All three act like an additional skin and reduce the permeability of the well; over a long period of time, this can lead to severe production losses. As a result, either costly and time-consuming well treatments have to be performed or, in the worst case, the well will have to be abandoned. To prevent these contingencies, different methods are used in the industry. Flushing the perforations with solvents or acids is a standard procedure but has several negative impacts, the most serious of which is the environmental issue of pumping chemicals into the wellbore, which can frequently results in a degradation of the crude oil. Furthermore, acids need to be neutralized after the main treatment with a post flush, where a neutralizing fluid is pumped into the formation. Therefore, Progress Ultrasonic AG uses a different solution for well stimulation based on ultrasonic cleaning. A wireline ultrasonic device linked to a surface generator is lowered into the wellbore and produces ultrasonic waves for a certain period of time to treat precipitations in the near wellbore zone. This is applied with great success under certain conditions, but there is always some room for improvement.

As a result of the combination of different pressures, temperatures, lithologies, fluids, impurities and even different completion methods, the task of making exact predictions regarding treatment behavior is complicated. Challenging these difficulties, Progress Ultrasonic AG in cooperation with the Chair of Petroleum and Geothermal Energy Recovery wants to build an apparatus to perform tests in the laboratory to enhance the method of ultrasonic treatment on plugged perforations under various conditions. History has shown that not every well can be treated with 100% success; therefore, a better understanding of the cleaning process is necessary. One cleaning effect resulting from the ultrasonic treatment is thought to be cavitation—that is, multiple bubbles forming at the contact area of solid and liquid—which is a complex and highly erosive phenomenon. The bubbles that are formed oscillate within their diameter until they implode. The extreme pressures and temperatures that occur during this process are responsible for removing the impurities. However, the process of cavitation strongly depends on the surrounding conditions. At atmospheric pressure, this effect is the driving force for the cleaning mechanism. At pressures above 20 *bar*, there will not be cavitation at all.

Conceptual Formulation

The focus of this master thesis is the study of ultrasonic wave behavior in different fluids at different pressure and temperature conditions. Furthermore different well conditions, especially completions should be evaluated.

Taking a closer look at the physical processes that occur during the treatment, laboratory tests are planned. In detail, the behavior of propagation and attenuation in fluids and rocks with a focus on the phenomenon of cavitation at higher frequencies will be discussed in this thesis. The goal is to develop a better understanding of this cleaning phenomenon under different conditions to improve the treatment efficiency of the ultrasonic wireline tool.

The appearance of cavitation also depends on different conditions like the kind of fluid in the well (density and viscosity are the main driving forces). For this, a borehole simulator is planned to simulate ultrasonic treatment in the laboratory. As in the field, elevated hydrostatic pressures, temperatures up to 100 ° and different fluids (from water to high-viscosity fluids) will be covered by that simulator during the testing procedure. Moreover, the implementation of a casing for the simulation should be considered in order to get closer to real field conditions. To monitor and evaluate the tests, hydrophones are planned inside the simulator, especially for measuring the attenuation of the ultrasonic waves. Furthermore, there will be the possibility to heat up the fluid in the simulator.

2 Theoretical Fundamentals

2.1 Downhole Completions

After drilling a well to its target depth, careful interpretation and consideration of the well test data is performed. This leads to the decision whether a production casing is set and the well will be completed or plugged and abandoned. The decision to abandon is made if there are no hydrocarbons in place or if they are not commercially producible at present. However, it is possible that a plug was set at some time in the past and later the production becomes economical with increasing gas or oil price.

If it is decided to produce, it has to be completed. This means that equipment will be installed in order to allow a safe and controlled hydrocarbon flow. Various types of completions are available depending on the characteristics of the well. The kind of fluids, diameter of the last section, flow rate and degree of compaction of the reservoir rock are only a few of the factors that must be considered when choosing a completion type. The aim is to find the simplest and lowest cost completion method to meet the demand of the well.

Open Hole Completion

An open hole completion (figure 1), where the production casing is set and cemented above the zone of interest is a common method in the industry. After cementing the last casing section, the reservoir is drilled and is ready to produce. However, in most cases, the hole is not left without any tubulars.

The advantages of high flow rates due to the larger open flow area and low costs are the main reasons for this type of completion. Furthermore, if a weak reservoir formation is expected, the high loads that occur during cementing do not exist. Even so, it still has disadvantages like controlling water and gas production, and hardly achievable selectivity for treatments or sand production.

The latter can be avoided by using a standard gravel pack or sand screen, as shown on the right in figure 1. Such screens hinder, for example, formation sand that was loosened by the fluid flow during production from entering the borehole and damaging the equipment. [1, p. 211]

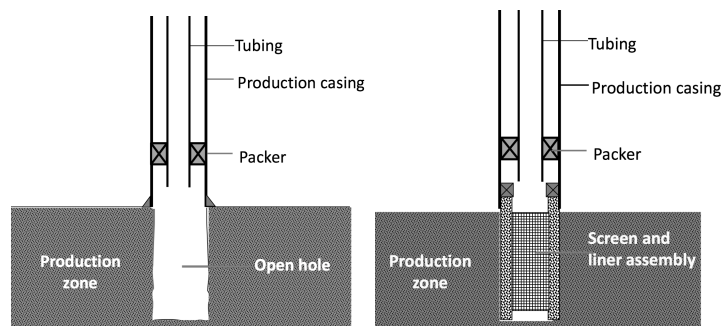


Figure 1: Open hole completion and screen completion [2]

Cemented Completion

In addition to open hole completion, there is the possibility to cement and perforate the reservoir section for better control of the producing fluids. Either a casing from the surface is run to target depth or only a liner is brought into position. They will afterward be cemented at reservoir depth, as is displayed in figure 2a. The liner can also be pre-drilled or slotted into the wellbore (figure 2b). In this case, no cementing or downhole perforation job will be performed.

In the case of cementation, a hydraulic connection through the steel body and the cement to the reservoir must be created to produce any hydrocarbons. A perforating gun is lowered into the well and fired; this blasts steel ends into the formation to create flow paths. Afterward, the tubing can be run and production can begin. It is also possible to produce without production tubing, through a process called tubingless completion. This is used in slim hole completions to gain additional flow area. However, it can lead to severe troubles if no tubing is installed and fluid is produced through the casing. Erosion and corrosion attack the inner casing wall and repairing a leaking casing would be a costly operation. [3]

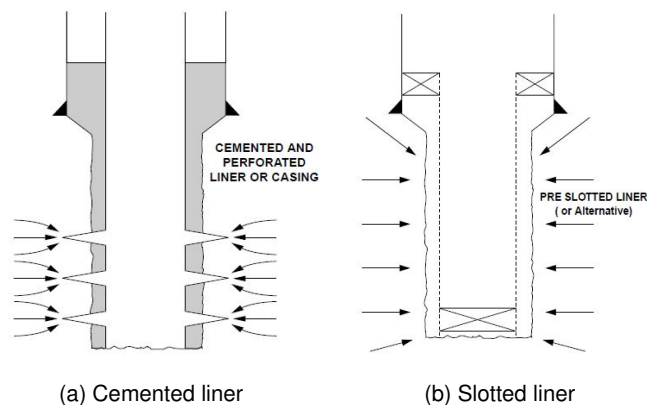


Figure 2: Cemented/perforated casing and pre-slotted liner [4]

2.2 Perforation Impurities

During the life cycle of a well, changes in pressure, temperature or chemical composition can lead to an unwanted side effect called precipitation. This can plug the formation (e.g. coat the grains) and reduce the permeability of the near wellbore area. This is called the skin effect and it causes an additional drop in pressure, thereby lowering the production rate. Losses running into millions of dollars are caused every year by unwanted precipitation of asphaltenes, paraffins and scale.

2.2.1 Scale

Scale is an assemblage of deposits that plug perforations as well as casing, production tubing, valves, pumps and downhole completion equipment, even surface equipment. For example, in home situations, like in the water kettle or home plumbing, scale can occur all along the route where water is flowing. In the petroleum industry, this phenomenon is related either to the water in the formation or to a mixture of incompatible waters (figure 3) that are being produced by hydrocarbons or injected water from the surface. This mixture becomes oversaturated with scale components and precipitation is the consequence. The resulting drop in pressure leads to even more precipitation in the formation matrix (figure 3, right insert). The amount of dissolved solids in water can thereby increase to $400,000 \text{ mg/L}$. At this level, scale reduces or even completely plugs the free flow area of the formation or the production equipment. [5, p. 31]

Scale consists largely of the minerals, calcium carbonate (CaCO_3) and calcium magnesium carbonate ($\text{CaMg}(\text{CO}_3)_2$). However, sandstone formation fluids often contain other elements, such as barium and strontium, but is not as typical for scale in the near wellbore area as carbonate or sulfate scale. These have finer particles and block gravel packs, screens and matrix pores. This can happen if the well is shut in for a longer period and incompatible waters are mixing. Even in areas like the North Sea or Canada, scale is recognized as one of the top production problems.

Therefore, inhibition is necessary but cannot always be performed. If so, a removal method like ultrasonic treatment is necessary. [5, p. 31]

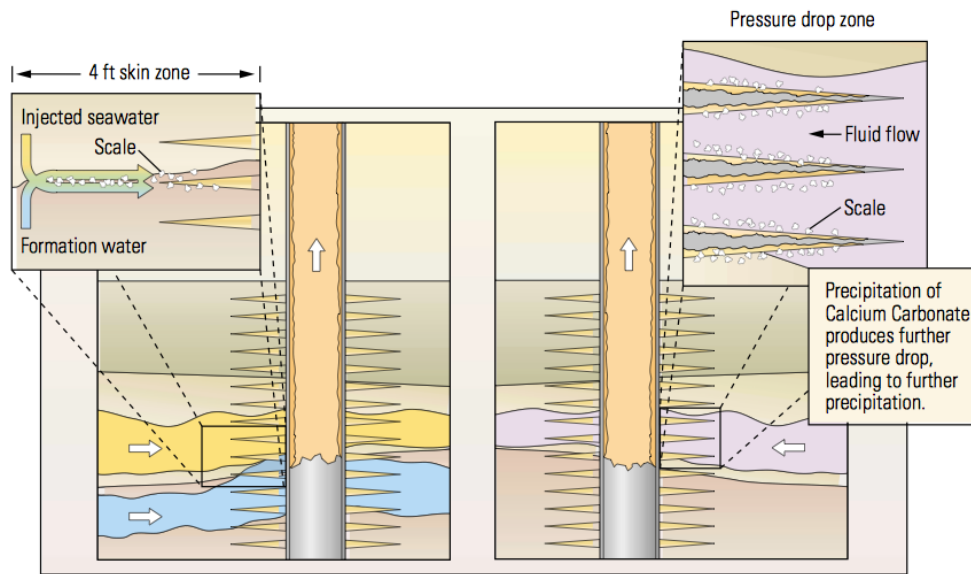


Figure 3: Production well damage due to scale [5, p. 35]

2.2.2 Paraffins

Paraffins are hydrocarbons with a molecular formula of C_nH_{2n+2} that align in most crude oils as long-chain molecules but can also form branched or cyclic structures where $n \geq 16$. A normal paraffin includes 16 or more (up to $C_{70}H_{142}$) carbon atoms forming a crystalline solid substance at 20°C , which is known as wax. Slight changes in the equilibrium conditions process can then lead to paraffin precipitation, which occurs in three phases. Let us begin with the *precipitation* of paraffins. The hydrocarbons emerge out of the solution and form suspended solids flowing along with the fluids. This *transport* process ends at pore throats, where the paraffin particles start to accumulate, thereby decreasing permeability (*deposition*, figure 4).

Even slight changes in equilibrium conditions, like pressure and temperature can start this process.

It is important to understand the temperature dependence because reaching the wax appearance temperature (WAT) leads to precipitation, especially in depleted reservoirs. Orthorhombic shapes are formed, thereby creating a stable three-dimensional wax crystal. [6, p. 2]

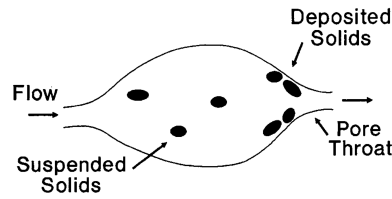


Figure 4: Schematic figure of paraffin deposition [7, p. 37]

Given that, in the same field, one well has wax problems and the next well does not, shows how sensible this precipitation process is. This experience contradicts the idea of one perfect solution for removing paraffins. Furthermore, removal operations could become more complicated if asphaltenes form part of the paraffin deposit. This is because many factors governing paraffin deposition also affect asphaltene deposition. Paraffins mostly deposit in near surface areas like wellbores, pipes and flow lines. [8]

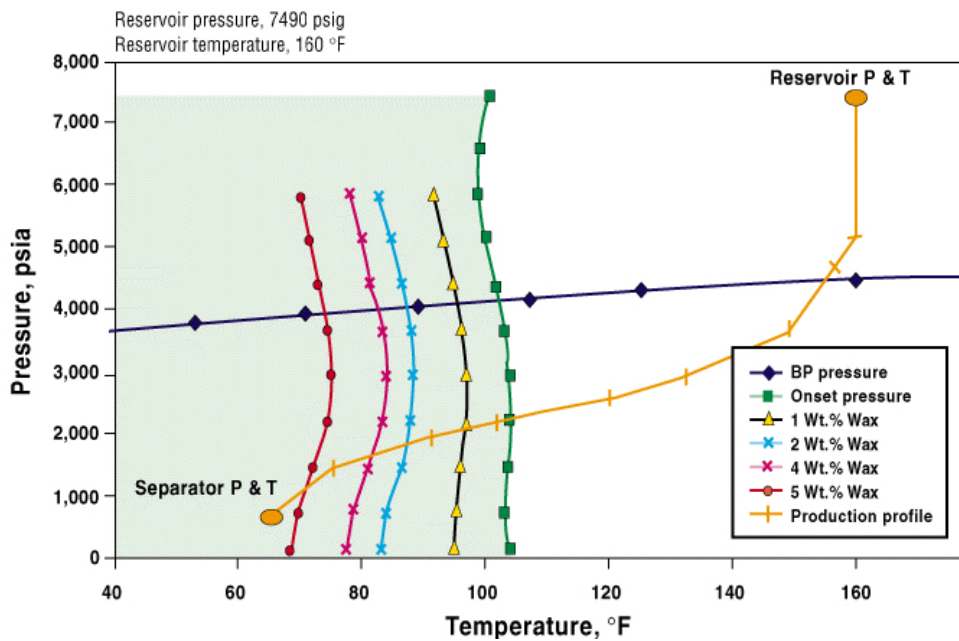


Figure 5: Wax appearance temperature (WAT) [9]

In figure 5, a typical wax precipitation envelope on a p-T diagram is shown. The green line is the precipitation curve and, to left (the green area), wax is precipitating. The colored curves in this example show the weight percentage of wax that precipitates from the oil. The black curve is the bubble point line of the oil. In contrast to the asphaltene precipitation envelope (APE in figure 6), the wax appearance curves are nearly vertical, which underlines the strong relation on the temperature in contrast to nearly no pressure dependence.

2.2.3 Asphaltenes

Asphaltenes are molecular substances that consist primarily of carbon, hydrogen, nitrogen, oxygen and sulfur. These stay dissolved in the crude oil flow as long as the pressure remains above the precipitation curve, which is called the upper asphaltene onset pressure or upper AOP (figure 6). If the pressure is lowered to the curve, first asphaltene precipitations show up. As the pressure decreases, more asphaltenes continue to form until the pressure reaches the bubble point line (figure 6). At this line, gas is forming. However, if enough is released, the gas starts to redissolve asphaltenes at the lower AOP (the pressure where the last asphaltene is dissolved). The redissolution can be very slow; therefore, the prediction of the lower onset pressure curve is hard to achieve.

The deposition of asphaltenes is also noted in wells that are CO₂ flooded, in miscible drive floods and after acid stimulation in production wells. This leads to the mixing of oil with incompatible solvents, acids and other hydrocarbon fluids. The formed asphaltenes, which are dark colored and crumply, are insoluble in n-alkanes, such as n-pentane, and soluble in toluene. Hence, a high asphaltic content does not strictly mean a precipitation problem. It also depends on the resin content in the oil. Resin is a hydrocarbon secretion of plants, which is generated particularly from coniferous trees. If the amount of resin is high, talking from a resin-to-asphaltene volume ratio from 1:1 to 20:1, the mixture is stable. Ratios of less than 1:1 characterize a rapid precipitation of asphaltenes, which have no defined melting point but decompose when they are heated. Asphaltenes can deposit everywhere in the production string, but induce most damage in the near wellbore area, reducing or even plugging the pore throats. Periodic intervention with solvent soaks or continuous injections of chemicals are performed for inhibition. However, this is effective only as the oil leaves the formation and moves into the tubing where the chemicals can interact. Instead, the inhibitors are squeezed into the formation after being pre-treated with an activator chemical. [11, p. 45]

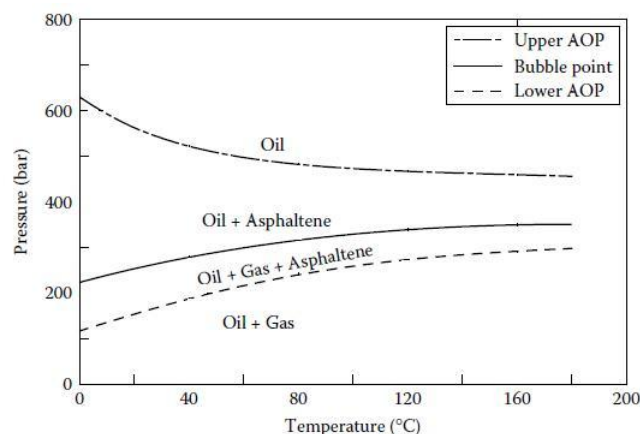


Figure 6: Asphaltene Precipitation Envelope [10]

2.3 Conventional Removal

2.3.1 Scale

The removal of scale strongly depends on the type of scale and the speed at which it can reappear. Chemical removal is often the first choice, especially in areas where mechanical removal cannot be applied. *HCl*, for example, is particularly suitable for the dissolution of carbonate minerals. Hard sulfate scale, however, has low acid solubility and is difficult to remove using hydrochloric acid. The addition of strong chelating agents, which break up the acid resistance by isolating and locking up the metallic ions within their closed ring-like structure, are used to enhance the effectiveness. The speed and the effectiveness are also controlled by the surface-area-to-volume ratio, indicating how well the reactant can touch the surface of the scale. In high-permeability zones, where paths of least resistance occur, the treatment fluid is hindered from penetrating the intervals damaged by the skin. In theory, scale is easily removable using acid treatment or chemical dissolvers, but in many cases it is not. Waxy or tar-like coatings hydrocarbons act as a protection for scale against dissolution by acids. [5, p. 42]

2.3.2 Asphaltenes

In the case of asphaltenes, a stabilization of crude oil by addition of an aromatic solvent (e.g. 10% Xylene for oil with 8% asphaltene) can be achieved. A much lower volume input is needed to stabilize the crude than it would be to solubilize completely all solid deposit. Hence, this is a possibility for handling problems with high asphaltic oils, but is not an alternative for focusing on their production. However, it offers advantages during treatments in combination with acids or other substances that lead to precipitation. A solvent where Xylene is dispersed in HCl showed, for example, significant improvement in stimulation in a controlled application of solvents within an asphaltic oil reservoir.

In contrast, the treatment of asphaltene works, as mentioned earlier, with solvents and co-solvents (mixtures of solvents, e.g. the combination of aromatic and straight-chain solvents with a small amount of hydrophylic solvent is often used). They dissolve and disperse asphaltene deposits and actually wet the surface involved in the reaction, but they need some time to react, which is called the soak time. After squeezing into the formation, they are left for 24 to 48 hours in the formation. Longer durations can result in severe damage of the formation. The amount of injected treatment volume varies from 5 to 50 gal/ft of the pay zone. [12, p. 395]

2.3.3 Paraffins

The removal of paraffins is dependent on the location of their deposition. The oldest removal method is mechanical removal using scrapers (figure 7a) for the tubing and pigs (figure 7b) for flowlines, but it cannot be performed in the case of impurities inside the formation matrix.

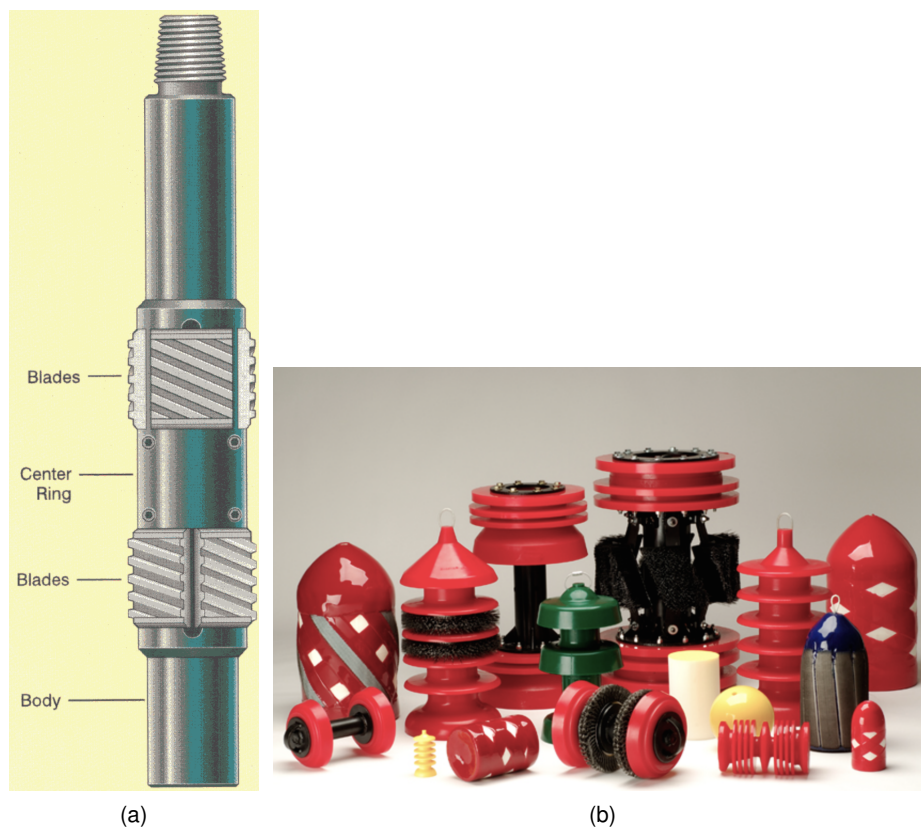


Figure 7: Casing scraper [13, p. 44] and pigs [14, p. 1] for removing precipitations

Another well-known method is the injection of hot fluids like oil, water or even steam into the formation to “melt” the hydrocarbon deposits. However, injection of hot media can lead to negative impacts on the formation, like wettability alterations, emulsion formation and mineral transformation in the manner of clay swelling. Moreover, the dissolved paraffins can redeposit in the formation when the injected oil is saturated with the melted paraffin and the formation temperature is lower than the cloud point of the oil. [15, p. 1]

The most popular method for removal of paraffins is, as for the asphaltenes, the usage of solvents. Carbon disulfide, for example, is one of the most frequently used chemicals for treating paraffin depositions, but it is extremely dangerous. It is explosive at -30°C (flash point) and has an autoignition temperature of 100°C . Furthermore, it is very poisonous for humans and, hence, is banned in most countries. Xylene and toluene are also effective solvents that are commonly used in the industry. Often, a large quantity is needed because they quickly reach their saturation point.

Dispersants are added to the oil or water before it is circulated. In order to remove paraffin deposits, they do not dissolve paraffin, but disperse it in the oil or water through surfactant action. [16]

2.4 Ultrasonic Waves

The term, ultrasonic waves, describes a vibratory wave with frequencies above the level of human hearing. This generally refers to frequencies of 20 kHz and more but the starting point is not clearly defined. However, there are ultrasonic applications using 15 to 18 kHz. From the physical point of view, there would be no need to distinguish ultrasonics from acoustics because the origin and propagation of sonic waves is independent of the frequency. Nevertheless, there is a major difference between the generation and detection of ultrasonic and acoustic waves, respectively. At high frequencies, every structural element of the transmitter has to be seen as a wave conductor and treated dynamically, which means that it cannot be treated like an elastic spring. Acceleration, alternating pressure, intensity and energy density are much higher in the case of ultrasonics as compared to acoustics at low frequencies. Consequently, those non-linear effects are becoming stronger that were up to that point negligible. Examples of this include acoustic radiation pressure and also cavitation, which will be described later on. [17, pp. 13-14]

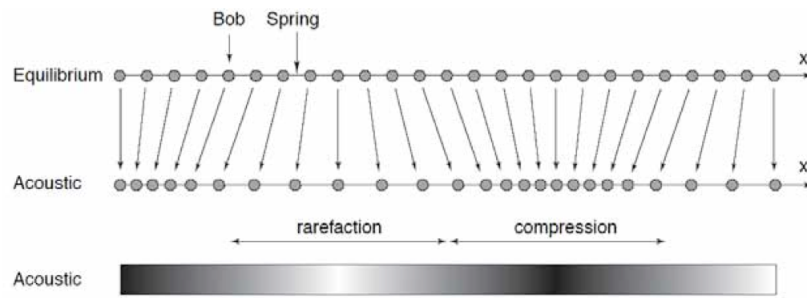
2.4.1 Generation of Ultrasonic Waves

The generation of ultrasonic waves in technical applications is, in most cases, based on the piezoelectric effect. It produces an electrical charge in certain non-conductive materials like quartz crystals and ceramics if mechanical stress is applied. This effect is fully reversible and, therefore, also able to generate vibrations when subjected to an alternating electrical field. Thereby, the material exposed to that field vibrates at a precise frequency with very little variation, which makes it very useful for technical applications. [17, pp. 81-82]

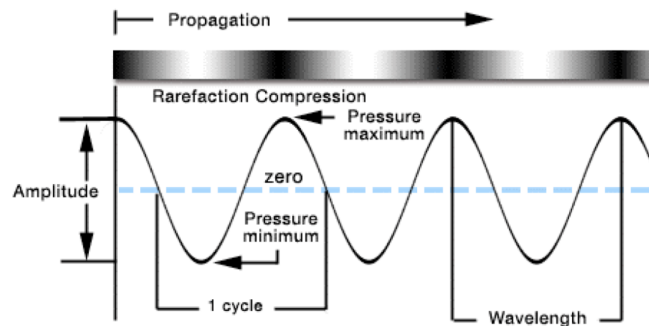
Sound waves

Sound waves propagate by longitudinal and transversal motion through solid materials. Fluids or gases can only transmit longitudinal waves because transversal waves propagate as shear waves only through a solid structure, as fluids are unable to transmit shear motion.

Sound waves are an alternating action of compression and expansion. This can be modelled as a system of weights connected by springs, as shown in figure 8a. At equilibrium, the distances between every mass element is exactly the same. Figure 8b implements the characteristics of the wave where the rarefaction is visualized as a bright area with the lowest pressure and the compression part as a dark area with the higher pressure. [17, p. 18]



(a) Mass - spring system



(b) Longitudinal wave

Figure 8: Propagation of a longitudinal wave through gases and liquids [18]

In contrast to fluids and gases, wave propagation in solids tends to be much more complex as a result of the form elasticity of the solid material. Therefore, a great variety of waves occurs, especially in addition to the longitudinal waves, transversal waves that are propagating through the solids. This becomes even more complex if the elastic constants and other physical characteristics of the solids are anisotropic. This means that the properties of the material depend on the direction. [17, p.18]

Acoustic waves in isotropic solids

In the case of a propagation in an isotropic solid and the wave assumed as plane (propagation in x-direction in this case), the wave can be described by equations 1 to 3.

$$(2\mu + \lambda) \frac{\delta^2 \xi}{\delta x^2} = \rho_o \frac{\delta^2 \xi}{\delta t^2} \tag{1}$$

$$\mu \frac{\delta^2 \eta}{\delta x^2} = \rho_o \frac{\delta^2 \eta}{\delta t^2} \tag{2}$$

$$\mu \frac{\delta^2 \zeta}{\delta x^2} = \rho_o \frac{\delta^2 \zeta}{\delta t^2} \tag{3}$$

Variables ξ , η and ζ are the components of the displacement vector, where ξ moves in the

same direction as x . The other two are perpendicular to the propagation direction x . Variables λ and μ are, in that case, coefficients of elasticity and are known as Lamé constants, which are not to be confused with the wave length. [17, pp. 38-39]

The first of the above-mentioned three equations describes, therefore, the longitudinal wave. By comparing this with the partial differential equation (4), the sonic velocity can be derived (equation 5).

$$\Delta p = \frac{1}{c^2} \frac{\delta^2 p}{\delta t^2} \quad (4)$$

$$c_L = \sqrt{\frac{2\mu + \lambda}{\rho_0}} \quad (5)$$

This is the fastest wave and is also known as the compressional wave or dilatation wave in contrast to the other two waves that describe the behavior of the transversal wave. This velocity is always lower than for the longitudinal wave. The velocity of the transversal wave can be calculated in the same way as for the longitudinal wave (equation 6).

$$c_T = \sqrt{\frac{\mu}{\rho_0}} \quad (6)$$

In figure 9, the propagation of the transversal wave through the material is visualized. During this propagation of the wave, the small elements (black squares) do not change volume as in the longitudinal wave, only the shape changes. For that reason, they are also called shear waves.

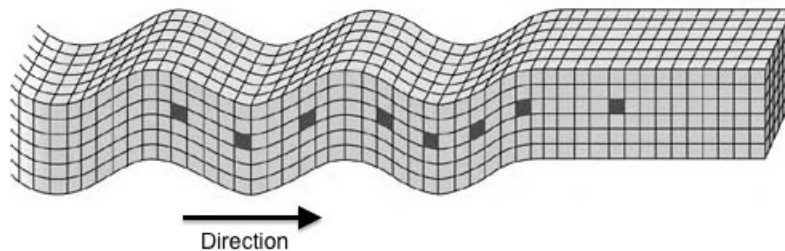


Figure 9: Propagation of the shear wave [19]

Another important characteristic of ultrasonic waves is the characteristic impedance, which is defined as the relationship between the acoustic pressure p and acoustic particle velocity v . This acoustic pressure is the difference between the absolute pressure and the pressure at rest. If no wave is acting, the absolute pressure would be equal to the pressure at rest; therefore, the acoustic pressure would be zero. Furthermore, the acoustic particle velocity is the velocity of the deflection of the wave. [17, p. 39]

The sonic velocity and the impedance vary with different media as shown in table 1.

Table 1: Physical parameters of gases and fluids [17, p. 25]

Media	Temperature (°C)	Density (kg/m ³)	Sonic velocity (m/s)	Characteristic Impedance (Ns/m ³)
Gases				
Air	0	1.293	319	429
Carbon monoxide	0	1.250	338	423
Carbon dioxide	0	1.977	259	512
Oxygen	0	1.429	316	452
Fluids				
Water	20	998	1483	1.48
Diesel oil	20	1250	1250	1.00
Benzol	20	878	1324	1.16
Methyl alcohol	20	1324	1120	0.89

Diffraction and refraction

If an acoustic wave travels through a liquid or a gas and hits a plane surface with different physical properties, it may be reflected partially or even totally. Hence, properties like phase and amplitude are changing, and the part of the wave that penetrates the surface can change the direction and the speed. This phenomenon is called refraction, but there is also the possibility that the wave is completely reflected or completely penetrating the other media. [17, p. 45]

In figure 10, the wave moves from one gas or liquid with the sonic velocity c and an impedance Z into another with c' and Z' .

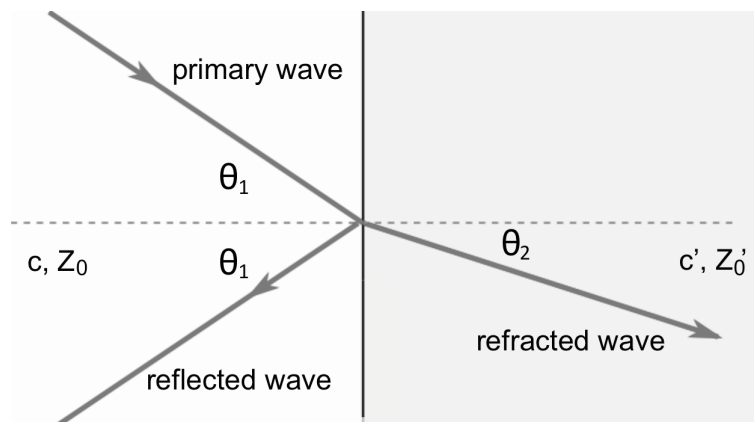


Figure 10: Diffraction and refraction of the incoming primary wave between two fluids or gases

Thereby, the angle of refraction can be calculated, as in optics, with the law of refraction (7), which says:

$$\frac{\sin \theta'}{\sin \theta} = \frac{c'}{c} \quad (7)$$

From this equation the angle can be calculated and if $c' > c$, then the angle of refraction will be bigger than the angle of incidence. The maximum thereby is 90° , which leads to a limited angle of incidence.

Take a look at the transition while considering that at least one of those two materials is a solid. It becomes more complex because even the solids transmit shear waves as mentioned earlier. Depending on whether one or both materials are solids, tangential forces on solid boundaries appear, distinguish or must be passed on. For that reason, the incoming longitudinal wave is partly converted into a transversal wave whereas the transversal wave creates a longitudinal wave at the interface. In the case of two force-fitted solids, each diffraction and refraction form, for a small angle of incidence, a longitudinal and a transversal wave. [17, p. 46]

2.4.2 Piezoelectric Effect

The piezoelectric effect is a useful application that is used for producing and detecting sound waves as well as generating high voltages and electronic frequency, among other things. The piezoelectric effect is caused by the asymmetry of the crystalline structure of the material, where one of the most important materials is quartz (SiO_2). Under stress, the elastic deformation of the crystalline structure leads the positive and negative ions to deviate from each other in such a way that every crystal element forms an electric dipole moment (figure 11). Due to alternating waves, the polarity changes, thereby inducing an electrical field that can be measured (receiver operation principle). [17, p. 87]

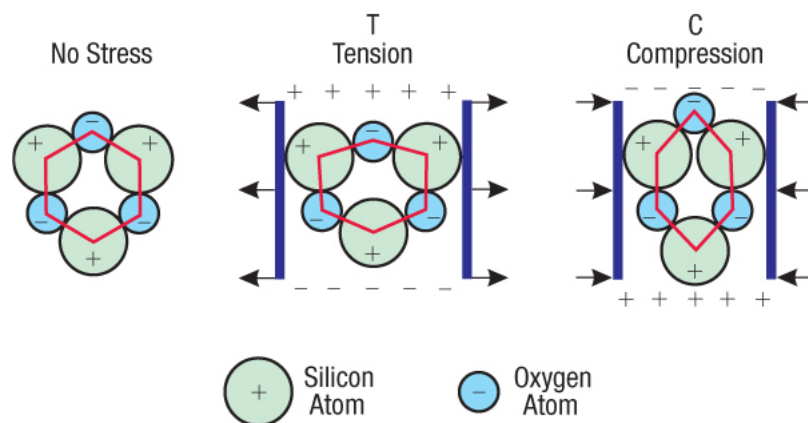


Figure 11: Dipole moment induced by mechanical deformation of quartz crystal [20]

This linear interaction between the mechanical and the electrical state is a reversible process. Applying an electrical field leads to a deformation of the crystalline structure and, therefore, to a mechanical force. With a fast changing electrical field, and the alternating compression and expansion, the material has become a transmitter.

Piezoelectric materials

Not every material is capable as a piezoelectric material. Such a material can be built from inorganic, organic or even from polymers or occur naturally. They can be grouped into: [21, p. 343]

- monocrystalline materials
- polycrystalline ceramics
- semicrystalline polymers
- cellular polymeric ferroelectric

To the group of *monocrystalline* materials belong naturally occurring materials like quartz or tourmaline, but also synthetic compounds like lithium niobate (LiNbO_3). The latter has a high Curie temperature of 1210°C and a very low acoustic attenuation, which is therefore used as the basis material in optical applications for surface waves for frequencies up to a few GHz. Quartz has extraordinarily good mechanical and electrical characteristics and is an important piezoelectric material, especially at frequencies above 10 MHz. Few mechanical and electrical losses, high dielectric strength and relatively low costs are the main advantages of this material. Furthermore, a high chemical resistance made it attractive for treatments in the oil industry, where many chemicals come along with the produced fluids or gases. Although quartz is used in the form of thin plates, its physical properties are highly anisotropic. It depends on how the quartz crystals are placed relative to the surface of the plate. In contrast to quartz, tourmaline responds equally to pressure from every direction and is, therefore, used for acoustic transducers in water.

Many piezoelectric materials are ferromagnetic, where the crystalline structure shows a high degree of symmetry above a certain temperature (the Curie temperature for quartz is 573°C). Below that temperature, the crystalline structure deforms by shifting positive and negative ions towards each other. This takes place in small domains in the same order forming a similar dielectric polarization in these small areas. If the polarization occurs uniformly, a strong piezoelectric effect can be achieved. [21, pp. 343-344]

Lead zirconate titanate ($\text{Pb}(\text{Zr}, \text{Ti})\text{O}_2$), abbreviated as PZT or PKT, is a material which is treated in that way. It belongs to the group of *polycrystalline ceramics* and starts to generate measurable piezoelectricity at deformations in the order 0,1% of the original dimension or conversely, the dimensions change 0,1% if an electric field is applied to the material. [22]

Materials like PKT, barium titanate (BaTiO_2) and lead niobium oxide (PbNb_2O_6) can only be produced as powder, not as uniform crystal. With this powder piezoelectric ceramics are produced in the way of mixing them with fluid binder material, pressing and sintering for different requirements. These ceramics later display small randomly polarized areas that neutralize each other. Afterward, the material is heated to above the Curie temperature of the raw material to force a uniform polarization with an electrical field in the order of $10\text{kV}/\text{cm}$. The electric field holds constant during a slow cooling phase to save the polarization (a process that is similar to the magnetization of a permanent magnet). [21, p. 344]

Semicrystalline polymers are high-degree polymers consisting of long-chained molecules. The most important of these is polyvinylidene fluoride (PVDF), which is shown in figure 12, where CH_2 and CF_2 molecules are alternating. These two molecules are bound together as a lamellar-shaped crystal with a uniform direction of the dipole moment. Unfortunately is the dipole moment from lamella to lamella different which makes a polarization like for polycrystalline ceramics necessary. This can be carried out at room temperature or at a higher temperature, but due to the long-chained molecules, a high electric field strength—typically around $100\text{kV}/\text{mm}$ —is applied. The advantage of these polymers are their strong piezoelectric effect, high shapeability and mechanical toughness. They can be manufactured in slim films of as little as $2\mu\text{m}$ thickness, which are used for hydrophones as ultrasonic transducers at frequencies in the range of MHz. [21, p. 345]

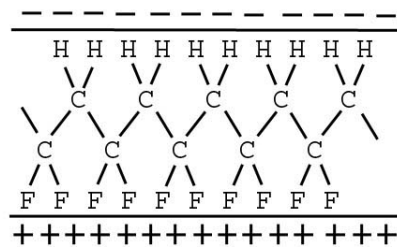


Figure 12: Chain structure of a PVDF crystal [23]

The latest group of piezoelectric materials constitutes the *cellular polymeric ferroelectric materials*. Cellular propylene (PP) is the most important representative of this group and consists of a closed polymer foam; 50% of its volume is occupied by gas bubbles. To polarize this material, the slim film is exposed to a direct current (DC) corona charging, which means that the surface of the film is strongly charged. Besides, the produced electric field inside the film discharges inside the gas bubbles and polarizes the margins, as is displayed in figure 13. [21, p. 346]

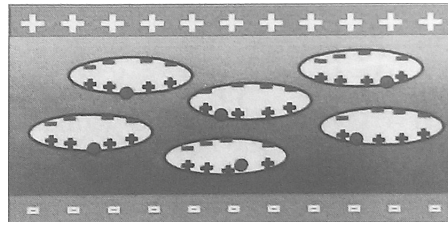


Figure 13: Charge distribution inside the film after treatment with the electric field [21, p. 346]

2.4.3 Behavior in Fluids and Gases

The usage of ultrasonics in different media shows different effects. In fluids and gases, in particular, the propagation of the ultrasonic waves is highly non-linear, which leads to different phenomena like steepening of the traveling wave and cavitation in fluids.

In the case of these non-linearities, the wave propagation velocity also depends on the amplitude of the wave. Positive pressure amplitudes travel faster than negative ones. The wave forms a shock front (figure 14) if it travels long enough. In most cases, however, especially under lower amplitudes, it is reduced by the attenuation. [21, p. 83]

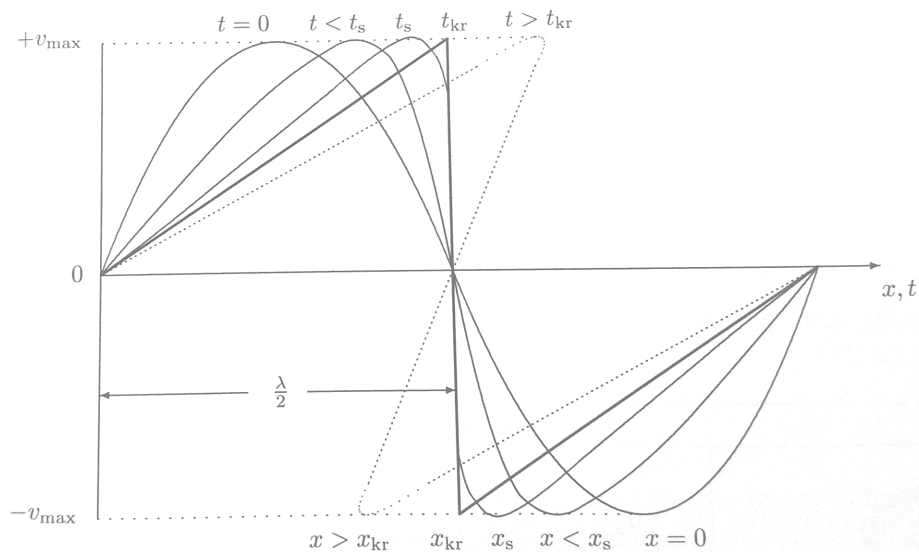


Figure 14: Sinus shaped wave which is steepening [21, p. 83]

The dotted line is only theoretically possible. In reality, it is physically unfeasible because it would require three acoustic field parameters (particle velocity v in figure 14) to exist for only one x value. Consequently the wave steepens up trying to form a perfectly sharp wave (figure 14, bold line).

The second phenomenon at high amplitudes is cavitation—that is, the formation of voids in a fluid caused by negative pressures. These voids do not last very long depending on the surrounding conditions, leading them to oscillate in size, shrink and implode with remarkable consequences. Cavitation is strongly non-linear and, therefore, also noted as an example for physical chaos. [17, p. 333]

Cavitation

Cavitation can be divided into two main categories:

- soft cavitation
- hard cavitation

Soft cavitation is related to gases that were previously dissolved in the liquid, such as air. At static conditions, the bubbles are spherical. Here, the pressure inside the bubble equals the gas pressure P_i and the pressure outside is the hydrostatic pressure P_0 plus the pressure from the surface tension σ of the fluid. [17, p. 334]

$$P_i = P_0 + 2\sigma/R_0 \quad (8)$$

The second term to be added to the hydrostatic pressure P_0 is called the internal pressure, where R_0 is the radius of the bubble. Since this pressure is higher than the external pressure, gas diffuses through the wall and the bubble shrinks until all the gas has escaped. At low intensity, the bubble oscillates with the same frequency as the sonic wave propagates through the fluid in a stationary field. This can be treated as linear so long as the amplitude is small. With increasing amplitude, the oscillation becomes non-linear with frequencies up to multiples of the sonic frequency. [17, p.335]

Hard cavitation is technically more important; hence, it is also called real cavitation. It shows smaller bubbles forming from the vapor of the liquid and not from dissolved gas as before. However, to generate vapor, the strong intermolecular attraction between the water molecules must be broken, which requires extremely high tensile force up to 300 bar negative pressure for pure water. Nevertheless, tests with tap water show bubbles forming already at a few bar negative pressure amplitude of the wave, which implies that other features must ease the generation of cavitation. [17, p. 345]

A concomitant phenomenon of hard cavitation is the cavitation noise that can be measured using hydrophones or even observed by ear to be an uncomfortable noise.

Cavitation nuclei

Let us first take a look at the related event of a boiling fluid. The formation of bubbles always starts at the bottom, similar to a soda bottle where the bubbles form either at the bottom or along the wall of the bottle. Examining such a bottle or a kettle under the microscope makes

it obvious that the surface is not perfectly smooth but, rather, has a certain roughness where micro-gaps exist. These are filled with gas, as is shown in figure 15 (also valid for microscopic suspended materials). [17, p. 346]

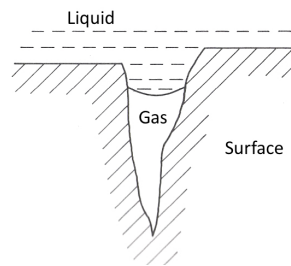


Figure 15: Gas filled micro gap on a solid surface [17, p. 347]

The boundary between the liquid and the gas is crooked and varies due to changes in pressure. With increasing hydrostatic pressure, the interface slants into the crevice to compensate. If this overpressure becomes static, the hole boundary moves into the crevices and the gas pocket shrinks (figure 15, dotted lines). On the other hand, the pressure can drop until a critical angle between the bubble and the gap edge is reached. At this point, the shape of the gas-liquid interface is no longer stable and a bubble leaves the crevice. This angle depends on how deep the liquid-gas interface has moved into the gap, which means that a longer static overpressure leads to deeper invasion and, therefore, the capability for lower pressure until the bubble leaves the crevice. [17, p. 346]

Behavior of a cavitation bubble

The process of cavitation is itself a cyclic process. Figure 16 shows the growth of a cavitation bubble in a fluid treated with sonic waves. In the upper figure, the sonic pressure is plotted where the first lower peak tears up the fluid bonding and forms a bubble (black dot in the lower picture). On reaching the positive half circle of the pressure wave, the bubble is forced to shrink whereas the diameter increases if the acoustic pressure turns negative. (see first picture in figure 16) This process is influenced by the inertia of the fluid. It slows down the shrinkage of the bubble and, therefore, the radius (lower figure) increases during the oscillation until the diameter reaches a critical value where the shrinking happens too fast to allow hindering them from imploding. A shock wave of the imploding bubble is the consequence. [21, pp. 90-91]

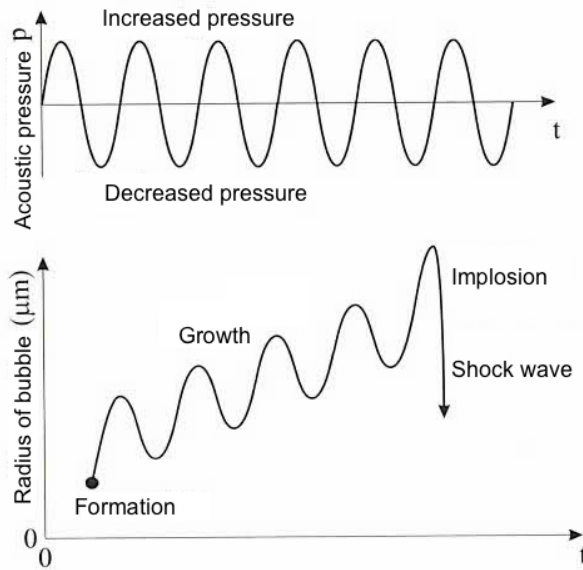


Figure 16: Growth of a cavitation bubble [21, p. 91]

Until this point, only one bubble was considered in the stationary field. However, hundreds of bubbles occur at the same time. The pulsation thereby introduces force of attraction between two bubbles, which is known as the Bjerknes force, where the supplanted and streaming fluids cause a negative pressure (Bernoulli formulated the occurrence of a decrease in the pressure of a streaming fluid). As a result, cavitation bubbles combine with each other, which is often followed by their splitting up again into two or more bubbles. [17, p. 352]

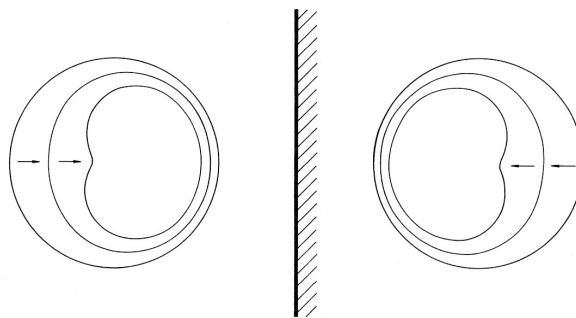


Figure 17: Deformation of the cavitation bubble in presence of a wall or another bubble [17, p. 353]

In the case of an implosion of the two similar bubbles next to each other, both are attracted by the implosion of the other one. The same applies to one bubble imploding in front of a solid (figure 17 with either two bubbles or one bubble and a wall). Due to force balance, the velocity component that is perpendicular to the surface wall cancels (or is removed by the same normal force from the second bubble). The originally spherical bubble becomes deformed because the side facing away from the wall moves faster towards the wall (deformation of bubble in

figure 17). The closer the bubble gets to the wall, the faster this happens until a small jet forms with velocities up to 400km/s (figure 18). [17, p. 353]

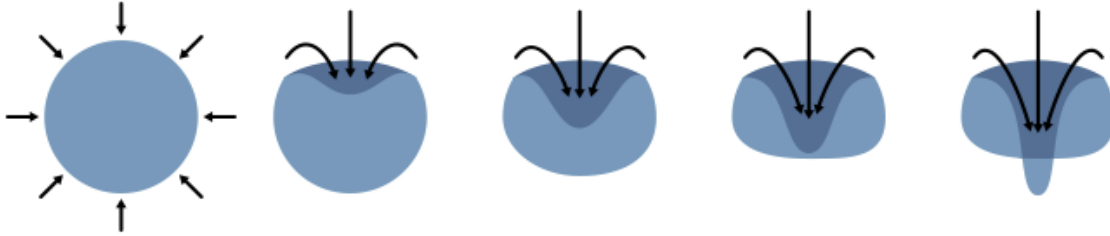


Figure 18: Formation of a jet [24]

This jet is one of the main causes of mechanical erosion due to cavitation. Soft materials like copper or nickel are particularly prone to erosion from cavitation. Another cause is the generation of extremely high pressures and temperatures when the cavitation bubble collapses. Based on adiabatic changes, the radius of a cavitation bubble can be calculated using equation 9. With an adiabatic constant for vapor in the bubble $\kappa = 1.4$ and a vapor pressure in the bubble $P_{i0} = 0.01 * P_0 = 0.01\text{bar}$, the radius of the bubble (R_0) decreases by a factor of 22 ($R_{min} = R_0/22$). [17, p. 355]

$$R_{min} = R_0 \left[1 + (\kappa - 1) \frac{P_0}{P_{i0}} \right]^{-\frac{1}{3(\kappa-1)}} \quad (9)$$

The maximum pressure can then be calculated using equation 10.

$$P_{max} = P_{i0} \left(\frac{R_0}{R_{min}} \right)^{3\kappa} \quad (10)$$

At the same time, the temperature increases during compression. Theoretically, it can reach the maximum value calculated in equation 11.

$$T_{max} = T_0 \left(\frac{R_0}{R_{min}} \right)^{3(\kappa-1)} \quad (11)$$

At the beginning of the implosion the temperature equals to room temperature ($T_0 = 293\text{K}$). During compression, the volume of the bubble decreases by a factor of 10760, thereby resulting in an increase in pressure by a factor of 441000. This means that the pressure increases from 0.01bar to 4410bar . Furthermore, the temperature increases by a factor of 41 and reaches 12000K .

As these are only theoretical values, they will not be reached in reality because the requirements for this equation become unfulfilled, especially during the last phase of the implosion. Nevertheless, they offer an indication of the extreme conditions to which cavitation can lead.

Besides, the effect of cavitation varies in different fluids. The strongest reaction is visible in water, whereas other organic fluids like ethanol mitigate the effect. First, those fluids have a higher vapor pressure that counteracts the surrounding pressure from outside the bubble and slows down the implosion. Second, the solubility of gas is much lower in water; hence, less gas diffuses into the bubble, thereby resulting in lower pressure at the beginning. Referring to equation 10, higher compressions and higher pressures are reached at the end. [17, pp. 356-357]

Furthermore, certain luminous effects accompany cavitation and are called sonoluminescence. This weak lighting is not continuous but, rather, takes the form of short lightings that occur during the last phase of implosion as a result of the extremely high temperatures. The level of intensity strongly depends on the fluids. Pure water, for instance, shows weak sonoluminescence. Nevertheless, if noble gases are dissolved in water, the intensity increases with the molecular weight of the gas. [17, pp. 359-360]

2.4.4 Attenuation

Up to that point, attenuation was left aside because the media was seen as ideal due to absence of losses. However, at higher frequencies, the effect of attenuation becomes very important. This is because of three physical processes where sound power and energy exponentially decreases the sonic wave. These are: [21, p. 35]

- inner friction
- heat transfer
- molecular absorption

The *inner friction* is considered with the dynamic viscosity where the attenuation constant α increases with the power of two and, as a result, it becomes extremely dependent on the frequency. In high frequency operations like ultrasonic treatment, the attenuation of 1 *dB* in air for 100 *kHz* is 0.5 *m*. Furthermore, the ultrasonic transducer can generate far higher frequencies of up to 20 000 *kHz*, where attenuation becomes very important. [21, pp. 35-36]

Attenuation through *heat transfer* is based on the assumption that the propagation of the sonic wave occurs adiabatically. Not only pressure and density, but also temperature changes between the two places. Those irreversible equalization processes also dampen the waves with the power of two, as for the inner friction. Since both have the same magnitude, Stokes and Kirchhoff brought both together in one equation and declared this to be the classic absorption effect. [21, pp. 38-44]

$$\alpha = \frac{1}{2\rho_0 c^3} \left(\frac{4}{3}\eta_d + \frac{\kappa-1}{\kappa} \frac{\nu}{C_V} \right) \omega^2 \quad (12)$$

In this equation, η_d is the dynamic viscosity, C_V the specific heat constant at constant volume, c the velocity of the sonic wave, κ the adiabatic constant, ω the sound frequency and ν the heat conductivity. [21, p. 43]

In terms of *molecular absorption*, the attenuation is based on the degree of freedom of the molecules. A stimulation of this movement needs energy, which results in a decrease in translational energy and dampening, respectively. [21, pp. 44-46]

2.5 Hydrophones

In order to gain results, the ultrasonic treatment must be recorded and, for this, implementing hydrophones will be necessary. Hydrophones are devices that are used to detect acoustic energy underwater by detecting pressure changes. In contrast to hydrophones, geophones detect motion rather than pressure.

2.5.1 Principle of Hydrophones

Hydrophones in active sonar systems are mostly used as both, projectors and hydrophones. However, there are reasons for separating hydrophones for reception—for example, to arrange them in towed line arrays for removing the ship's self-noise.

They detect the pressure variations of acoustic signals and noise in the water. This incoming signal is transformed to an output voltage that is proportional to the pressure. Additionally, the thermal agitation generates a noise voltage at any internal resistance. Consequently, the performance criteria for hydrophones are quite different from those for projectors. Projectors are usually operated in the vicinity of resonance with power output being the major concern. Nevertheless, hydrophones are usually operated below the resonance and the major concerns are the signal-to-noise ratio and the open-circuit output voltage. Hence, the smallest signal that can be detected by the hydrophones is a signal that is slightly less than or equal to the ambient sea noise. However, this is true for only as long as the internal noise of the hydrophone plus the preamplifier input noise does not exceed the sea noise. [25, pp. 152-153]

Piezoelectric ceramics are the dominant material in pressure-sensitive hydrophones because they have a flat response below resonance. Furthermore, as already discussed, piezoelectric ceramics can be pressed into various shapes and sizes that become, in combination with suitable electrodes, electrical cables and waterproofing for a hydrophone. [25, p. 154]

Sensitivity

Hydrophones made from piezoelectric materials are sensitive to pressure. Their sensitivity can be considered in terms of the acoustic particle displacement, which accompanies the low pressure that they are designed to detect. Having a look at the spectrum pressure level of sea state zero ambient noise, which is 44 dB at 1 kHz, the pressure is equivalent to 160 μPa . This pressure would lead in a plane wave signal to a particle displacement of 0.00017 *Angstroms*, which is equivalent to $1.7 \times 10^{-14} m$. The plane wave signal induces a displacement of the sensitive surface of the hydrophone, which is smaller than the displacement in water, as a consequence of the higher stiffness of piezoelectric ceramics compared to water. This small displacement is about 10,000 times smaller than the crystal lattice dimension and is detectable by the hydrophone. [25, p. 154]

2.5.2 Conventional Hydrophones

Cylindrical and spherical hydrophones

In the industry, circular, cylindrical and spherical hydrophones are the most used designs. Their high sensitivity, good hydrostatic pressure capability and simplicity are the main reasons for their widespread use. Moreover, to ensure a wide-band smooth response up to and possibly through resonance, having low impedance is generally a big advantage.

Spherical hydrophones need encapsulation to prevent water leakage while cylindrical ones additionally need end caps (figure 19). These are isolated from the tube and made of a highly compliant material like corprene, which is suitable for ambient pressure down to 300 *psi*. [25, pp. 162-163]

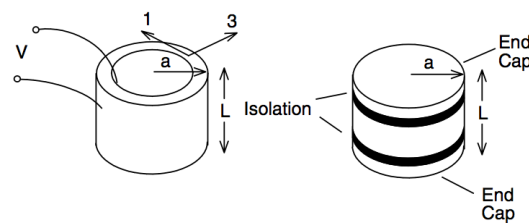


Figure 19: Piezoelectric ring with isolated end caps [25, p. 163]

In the figure above, a piezoelectric ring or tube is shown with a mean radius a , wall thickness $t < a$ and a length of $L < 2a$ with electrodes on the inner and outer cylindrical surfaces. It is polarized in the radial (3) direction and operated in 31 - mode. [25, p. 163]

Planar hydrophones

This type of hydrophone is typically used in closely packed sonar arrays. The transducer is usually designed as projector in active arrays, where the projector is also used as hydrophone. Using this, the maximum source level can be achieved and the resulting hydrophone response is usually found to be adequate in the active band. However, its use as a passive array outside the active band may not be satisfactory.

Some sonar scanning systems require a narrower receive beam than project beam. Therefore, a separation of projector and hydrophone arrays is needed, allowing a different hydrophone design in comparison to the projector design. For example, hydrophones may be operated below resonance, which provides less phase and amplitude variations from the hydrophone to the projector in the active band. The amount of piezoelectric ceramic material that is required may be much less for the hydrophone. Another advantage is an improvement of the efficiency to reduce noise in a separate receiving array to a projector array.

Figure 20 provides an example of a planar hydrophone. This tonpiz piston hydrophone has a length L , a cross sectional area A_0 , a piston head mass m_h , an input area A and a tail mass m_t . [25, p. 168]

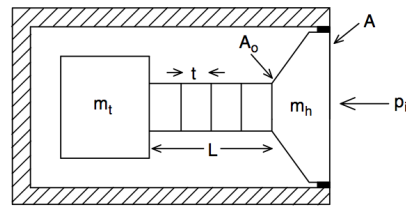


Figure 20: Tonpiz piston hydrophone with piezoelectric stack [25, p. 169]

Bender hydrophones

The bender is a device that derives its name from the action of bending. It is similar to the device in a bimetal thermostat. The bilaminar structure of the bender produces the action electrically.

Woollett developed basic treatments for disk and bar benders, which defined the influence of the diaphragm support, the dimensions and the choice of material. However, in the past, there has been an increasing interest in switching to flex-tensional types of transducers. Figure 21 shows a disk hydrophone supported on brass plates that are mounted on a brass ring. Encapsulation is also necessary to provide waterproofing for practical uses. The bender can be used as both, projector and hydrophone; the latter is achieved by sensing the electrical output that is produced by the pressure wave-induced flexure of the diaphragm. [26, pp. 174-175]

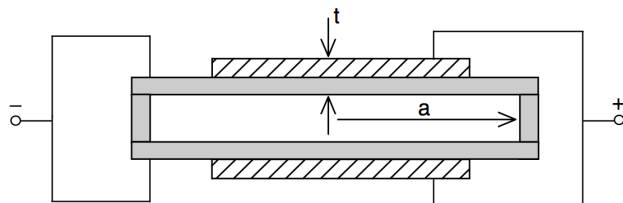


Figure 21: Simplified dual bender piezoelectric disc hydrophone [25, p. 175]

Studies on that device have led to the development of transducer designs that achieved among the highest output power observed from all types of transducers of the same volume or mass. [26, p. 175]

Vector hydrophones

Usually, piezoelectric ceramic hydrophones detect the acoustic pressure, which is a scalar quantity. This pressure is then converted into a proportional voltage. The pressure does not show a directional sensitivity if it is small compared to the wavelength. However, these acoustic sensors are sensitive to the magnitude and the direction of the wave; therefore, they are referred to as vector sensors. The ability of vector sensors to gain information from compact single- or dual-element hydrophone designs is the main point of interest.

Below resonance, the response of those vector sensors decreases with a decrease in frequency at a rate of 6 dB/octave and a 90° phase shift relative to the response of a pressure hydrophone. A relatively large equivalent self-noise pressure and a signal-to-noise ratio can be the consequence of the reduced sensitivity at lower frequencies. [26, p. 176]

2.5.3 Optical Hydrophones

Distributed feedback fiber laser

In the past, fiber optic hydrophone arrays based on interferometric sensors featured advantages compared to conventional piezoelectric hydrophone arrays. Factors like decreased weight and size, simplicity of design and operation, low power telemetry and high reliability pushes the development of these fiber optic hydrophones. However, with the rise of earth-doped fibers and improved in-fiber fabrication techniques, this distributed feedback fiber lasers, or DFB fiber lasers, have raised to a key technology. This has led to a new generation of fiber optic hydrophone arrays with reduced size, costs and complexity.

These DFB fiber lasers are made from writing a Bragg grating into an optically active material in an in-fiber device. For example, an erbium-doped glass is used, which is energized by intra-fiber optical pumping. Thereby, the frequency of the light produced by the fiber laser is extremely sensitive to small perturbations from the surrounding environment. Experiments underlined that measurable frequency fluctuations are induced by acoustic disturbances in the locality of the last cavity. They can be detected via interferometric methods, where two waves of the same frequency are combined and the resulting pattern is then determined by the phase difference. In general, phase sensing that is based on interferometric methods provide the highest sensitivities. The acoustic sensitivity can be explained with the extreme sensitivity of the laser regarding strain. In a well-configured system, this sensitivity of the fiber laser is limited only by the frequency noise of the laser. This is in the order of $20 \text{ Hz}/\sqrt{\text{Hz}}$, which is equal to a minimum detectable strain of 10^{-13} . [27, p. 1]

However, the bare DFB fiber laser, as shown in figure 22, is not well suited for pressure sensing. This is because of the relatively low direct pressure sensitivity and the tendency to respond strongly to local acoustic and mechanical vibrations. Therefore, for the construction of such a hydrophone, a mechanical support for the fiber to enhance its pressure sensitivity is necessary. This minimizes its response to other environmental perturbations, such as mechanical acceleration. [28, p. 629]

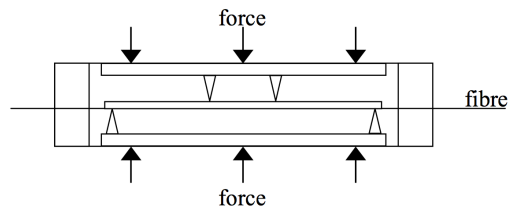


Figure 22: Operation principle of the DFB fiber laser hydrophone [28, p. 629]

Figure 22 displays the operation principle. The fiber laser is attached to one side of a flexible beam. This beam has an air-filled cavity that sits in the interior of the housing. For a beam thickness t , the core of the fiber bends from the neutral axis by a distance of $t/2$. This leads to a strain of $\varepsilon = t/2R$ on the fiber laser (R is the bend radius of the beam).

The acoustic pressure that is applied to the outer housing, causes the beam to bend and supports it, thereby imparting strain on the laser and resulting in a wavelength shift. The construction of the hydrophone assembly is comparable to a mechanical actuator, where external pressure is converted to longitudinal strain. The high flexibility and low inertia of the fiber allows it to move in accordance with the beam with little mechanical impedance. [28, p. 629]

Photonic crystal microphone

This kind of optical hydrophone was developed at Stanford University and it introduces a hydrophone with extraordinary features. In figure 23, an exploded view of the sensor head architecture can be seen. It consists of four different single-mode fibers, each of which brings in and returns a different optical signal. Three of these lead to a photonic-crystal diaphragm that is placed on the tip of the sensor head (a). The photonic crystals are high-reflectivity mirrors with an efficiency of more than 95%. The tips of the fiber are coated with a stationary mirror and each forms a Fabry-Perot interferometer when placed in close proximity ($25 \mu m$) with the photonic crystal. These three Fabry-Perot sensors are implemented on an area of 2.5 mm diameter. This is an order of magnitude smaller than the shortest acoustic wavelength of interest, which is 15 mm at 100 kHz , resulting in approximately the same acoustic amplitude. Thus, all three diaphragms have different diameters, starting from $150 \mu m$ over $212 \mu m$ up to $300 \mu m$ (figure 23 (a)); hence, all have different relative compliances ($\times 1$, $\times 4$ and $\times 16$). As a result, they are addressed to different ranges of pressure to increase the dynamic range of the sensor in contrast to a single sensor. The range of the pressure that can be recorded starts from the ocean's thermal noise ($\sim 10 \mu Pa/\sqrt{Hz}$) and extends to as large as 1 kPa . In other words, it covers a range of 160 dB , from a soft whisper in a library up to a ton of TNT exploding just 60 feet away. [29, pp. 5-6]

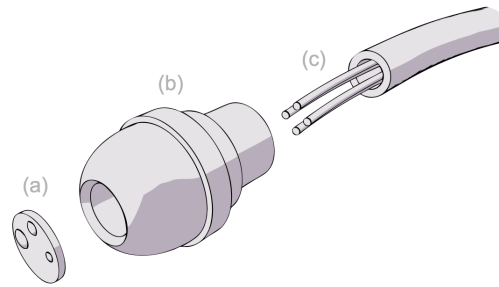


Figure 23: Exploded view of of the sensor structure [29, p. 5]

The fourth fiber is, for calibration purposes, connected to a reference reflector, which provides a static reference signal that accounts for noise and loss associated with the path through which the signals travel. However, the hydrophone must be protected against corrosion and dirt during operations in seawater. This is carried out by filling the sensor head with clean water. [29, p. 6]

Nevertheless, a diaphragm cannot move against a closed cavity that is filled with water, due to the extremely low compressibility of water. Hence, a small channel in the head is constructed; the water then flows through this channel into the surroundings and allows the diaphragm to move. In figure 24, a cross-sectional view of the sensor head is presented. The channels connecting the back chamber to the chip are fabricated around the fibers. The channel of the fiber defines the diameter of the diaphragm. All these channels differ in size; the biggest is the back chamber connection with a diameter of 1.5 mm . Furthermore, the back chamber occupies the most of the sensor head and is made of a water-filled cylindrical brass structure. The expanded channel has a diameter of 1 mm and can be seen in the lower right picture. [29, p. 6]

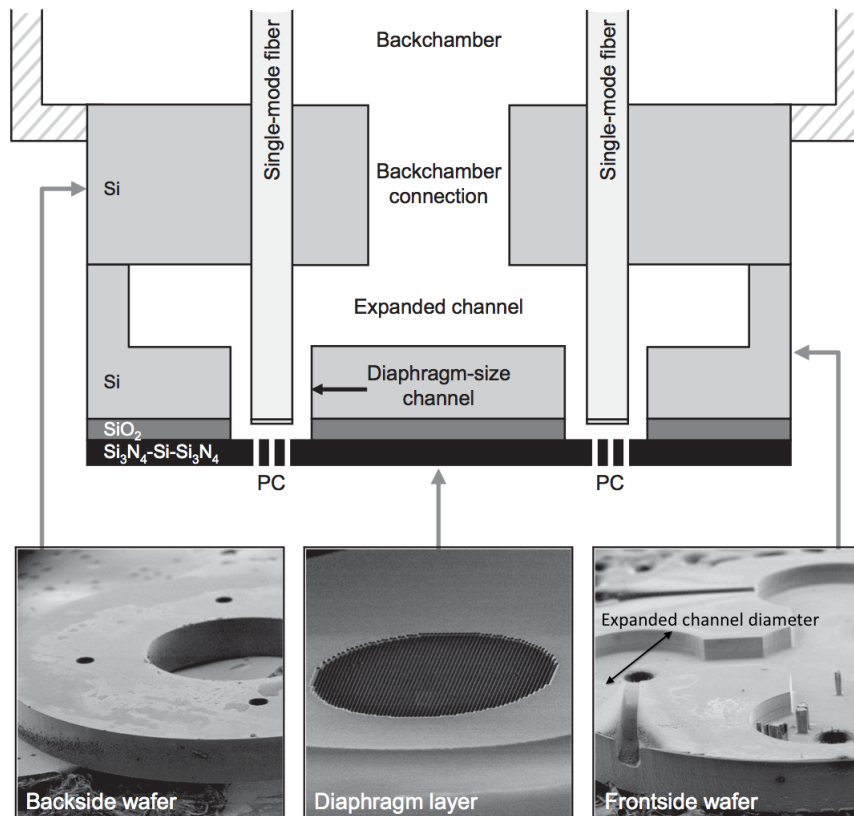


Figure 24: Cross section of the sensor chip with details of the parts [29, p. 6]

3 Borehole Simulator

3.1 General

In order to the shrinking development of new conventional hydrocarbon fields, the task of enhancing the production life of a field has become more important than ever. This means not only exploiting new or unconventional reservoirs like gas hydrates or shale gas but also increasing the recovery factor of existing and already abandoned reservoirs, respectively. Hence, an average recovery of about 30–35% of hydrocarbons that are brought to the surface leaves enough space for future technology to be applied.

However, enhancing the flow behavior and, therefore, the recovery factor of producing wells is a tough challenge. Accompanying effects during production of the already discussed perforation impurities decrease flow rates or even completely shut down the production. In order to prevent this, treatments like acidizing, scraping or ultrasonic cleaning are performed. Progress Ultrasonic AG specializes in the latter. To ensure further improvement, this company in cooperation with the chair of Petroleum and Geothermal Energy Recovery plans to do a construction for testing purposes; specifically, they want to construct a borehole simulator for ultrasonic testing in the laboratory. This simulator will reconstruct downhole conditions as closely as it is technically and ergonomically feasible. The ultrasonic test device used for this purpose is described in the next chapter.

3.2 Ultrasonic Wireline Tool

This method based on acoustic stimulation technology consists of the processing of a formation using aimed ultrasonic treatment. It is applicable for open hole, filter intervals or cased and perforated downhole completions. For the downhole treatment, an ultrasonic wireline device is used. An electric current generator that uses more than 18 kVA to power an ultrasonic generator is linked via a logging cable with a resonator. The frequency ranges of the treatment can be varied from infrasonic (1 – 100 Hz) up to ultrasonic in the range of 20 kHz . The device can be run from a depth of 200 m down to 7000 m and is carried out point wise in the well; the transducer can withstand temperatures up to 125 $^{\circ}C$ and a maximum pressure up to 500 bar .

One big advantage of this equipment is that it can be run in coordination with the regular equipment of geophysical parties without causing any difficulties in its adaptation by the regular geophysical personnel. Moreover, the well preparation is nearly identical to normal geophysical measurements. A sketch of the operation principle can be seen in figure 25.

Another point is that this technology can be carried out in a chemical-free manner or combined with standard methods from the industry (HCl treatment and others) that expand the application range and increase its effectiveness. [30]

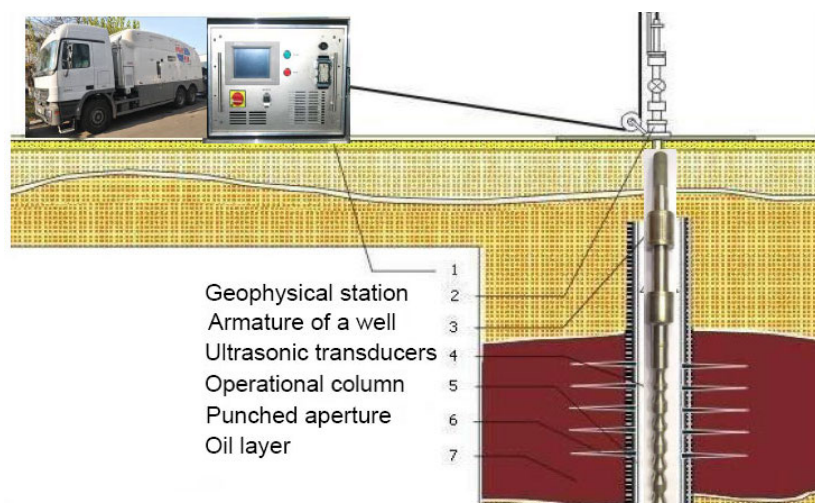


Figure 25: Construction of the ultrasonic wireline tool [17, p. 353]

The resonator comes in different sizes ranging from 1 3/4" to 3" with a maximum length of 1.8 m. During ultrasonic testing, the resonator must be fully immersed to achieve meaningful results, which requires a minimum height of more than 1.8 m.

3.3 Simulator Design Concepts

The overall design of the simulator is adapted to different requirements. These have been discussed with the company and must be considered in the planning phase of the simulator.

- three different completions must be planned for testing
- all resonator sizes have to be tested in this simulator
- the key area influenced by the ultrasonic waves are the perforations
- attenuation should be recorded
- immersion of the resonator in different fluids
- temperature increase must be measured

Completion methods were discussed early on in the thesis. Based on that, three different completions were chosen. In the first of those three, a perforated casing is planned since the steel body of the casing shields the formation best from the ultrasonic waves of all possible completions. The second method is the open hole completion. In contrast to the cased hole, the resonator is, via fluid, directly coupled to the formation and the ultrasonic waves can directly enter the formation. The gravel pack represents the third completion method and stands in between the previous two.

As mentioned above, the length of the resonator can extend to as much as 1.8 *m*. Therefore, the height of the planned simulator must be more than that to ensure full immersion.

The strong attenuation of the ultrasonic waves through the material leads to a focus of the treatment on the perforations and cement sheet, respectively. The same things take effect in the simulator. Therefore, the lithology behind the cement sheet will be replaced by cement with a certain permeability. This has several advantages, including reproducibility if the "formation" is damaged.

For every analysis, data is needed. Hence, for recording during treatment, the use of hydrophones is planned on the circumference of the simulator. The distance to the well can be varied by using cemented cable tracks. These should also hint at the strength of the attenuation in the different completions. This attenuation will also be influenced by the different fluids, as discussed in chapter 'behavior in fluids and gases'. The focus will be on water, oil and drilling mud but also on other fluids that are capable for the testing.

During the ultrasonic treatment, the increase in temperature should also be recorded; this will be done with a thermometer. The possibility of a liquid throughput would thereby open up more opportunities in this respect. Heating the treatment fluid before pumping it into the simulator could be a factor for ensuring more accurate real-field conditions. Furthermore, the increase in flow rate could be measured to ensure recording improvements during the ultrasonic treatment.

However, the key influence areas of the treatment are the borehole and, if there are any existing, the perforations. The influence of the hydrocarbon-bearing formation is, in that case, negligible and is replaced in the simulator by cement. The cement would be required for the completions anyway and has the advantage that it could be reproduced in case of damage.

Considering all those points, two early drafts were made:

Concept 1

The first concept covers the major points that were discussed with the company. As there are, fully immersion in fluid with different completions, where the attenuation is measured and recorded at variable temperature. Basically, it is planned as a borehole sample implemented into a steel pipe. The borehole completions are cemented into this steel pipe but every completion is cemented in a separate pipe. There are several reasons for this. First of all, in order to ensure reasonable and reproducible results, the measurement must be concentrated only on one completion per treatment. Furthermore, putting all three completions in one pipe would require at least a 6 *m* steel pipe (longest resonator has almost 2 *m*), which is economically unfeasible. Finally, implementing three different completions in one casing is very hard to achieve from the technical point of view.

For both concepts, the temperature is an important factor. At room temperature, heavy oils can have a honey-like viscosity. However, at reservoir temperature, the viscosity can be very low.

For the first concept, the process of heating is conducted by using a heating element. This will be put into the casing and the fluid inside will be heated up before the main treatment starts. For measuring the temperature, two possibilities are available: It can be measured immediately before and after the treatment or throughout the whole process.

In the figure below, the first completion is shown. It is a perforated casing cemented into a steel pipe body. The diameter of the casing is 5" and the steel pipe body has a length of 2.1 m.

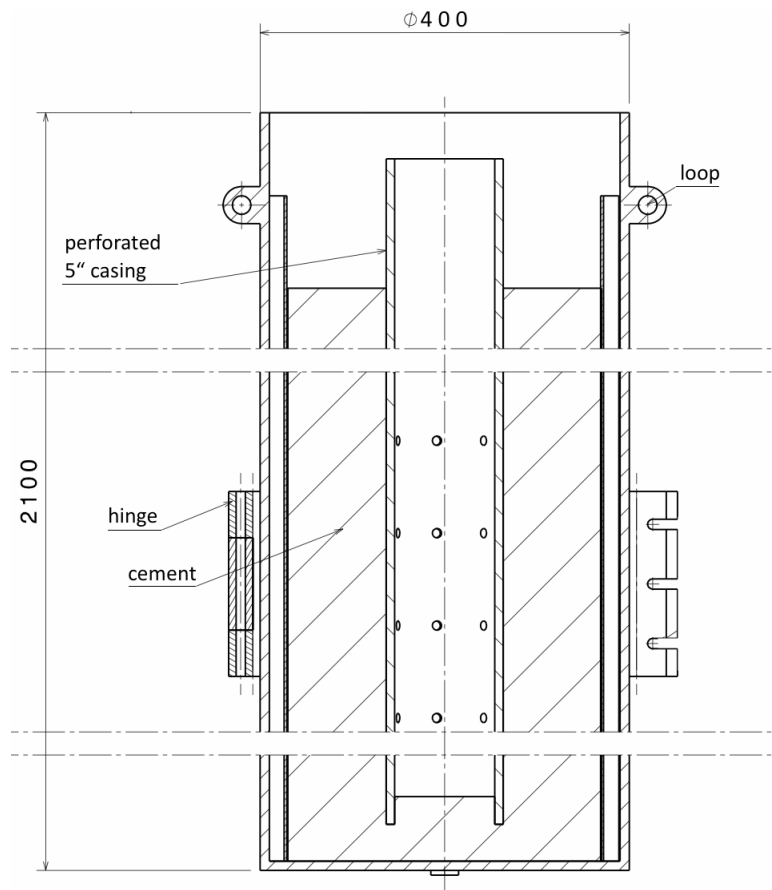


Figure 26: Example of a perforated casing completion in the simulator

The diameter of the simulator is about 400 mm. On the right side of figure 26, two loops can be seen. These are planned for the lifting operation. Since the height is more than 2 m, there will be about 300 kg of cement in one simulator, which makes handling without a elevator impossible. Furthermore, a hinge forms a separate tool of the simulator. It is marked and explained in figure 27.

The other completions (open hole and gravel pack completion) are performed in a similar way. The cement also replaces the formation of a borehole. However, creating an open

hole completion introduces difficulties. To produce it, a core has to be taken which must be removed after cementing. Therefore, a strong bond between the cement and the core must be avoided by using a thin plastic layer along the boundaries. In the case of the gravel pack, the gravel and the screen must be inserted after removing the core.

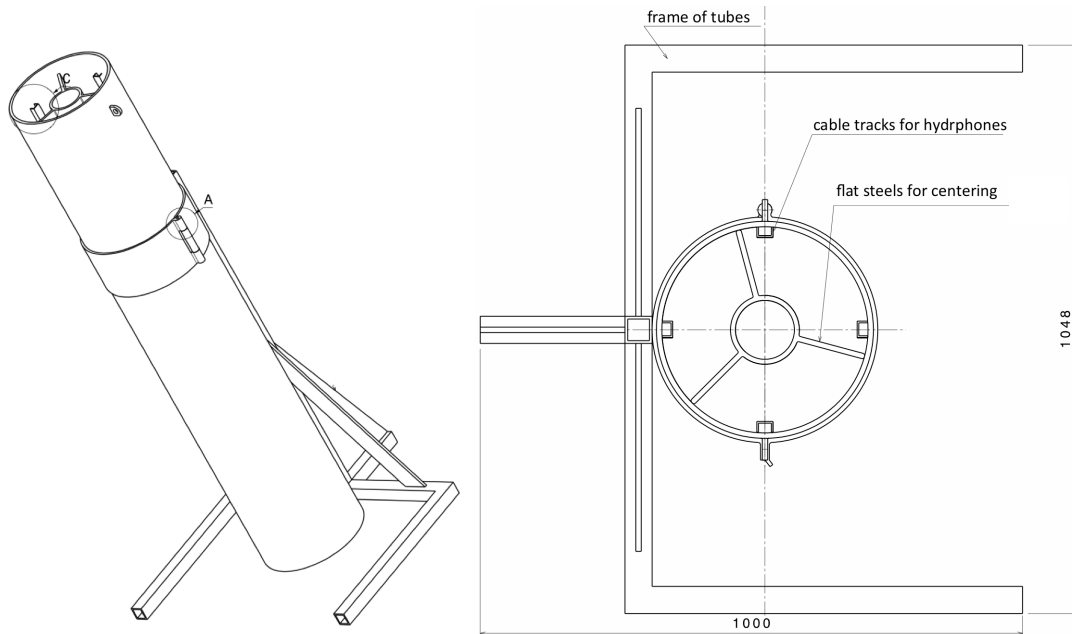


Figure 27: A 3D view of the simulator with the the closed hinge

This hinge (figure 27, detail A) is part of the frame for the simulator, which protects the simulator from falling. The frame is built from tubes that are welded together. It can be placed within the standing simulator and closed using the hinge and three screw connections (figure 28, left side).

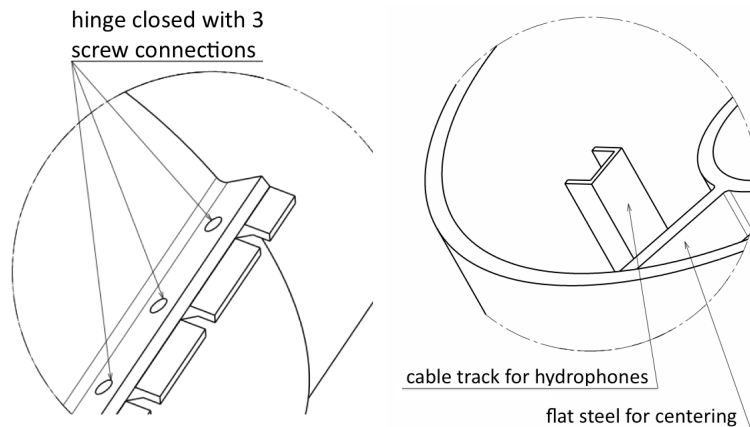


Figure 28: Details from the hinge and the cable tracks

On the right-hand side, the cable tracks for the hydrophones can be seen. They can be cemented in any distance from the center. Using different clearances, the attenuation through the cement can be determined. Furthermore, flat steel is welded on to the perforated casing to center it during cementation.

Moreover, this frame can be used for all three simulators (perforated casing, gravel pack and open hole completion).

Concept 2

Based on the first concept, a second concept was developed, focusing on the problem of elevated temperature and pressure. These two factors should be as close as possible to real field conditions, which indicates temperatures of up to 100 °C and pressures of a few hundred bar. The latter is tough to generate in such a big laboratory device and will, therefore, be the limiting factor for the construction.

To recognize improvements during the ultrasonic treatment, the idea of a liquid throughput came up. This would have the advantage that a change in flow rate and a change of the pressure drawn down through the “formation” can be measured and evaluated. However, to realize this goal, some parts have to be added.

Basically, the internal parts (completions, cement and the cable tracks) are identical to the first concept. The steel pipe from the first concept now has an additional function. As in figure 29b, this pipe is now perforated to form a hydraulic connection with the cement. This perforated pipe is inserted in the second pipe (figure 29a). The two are sealed and screwed in place together.

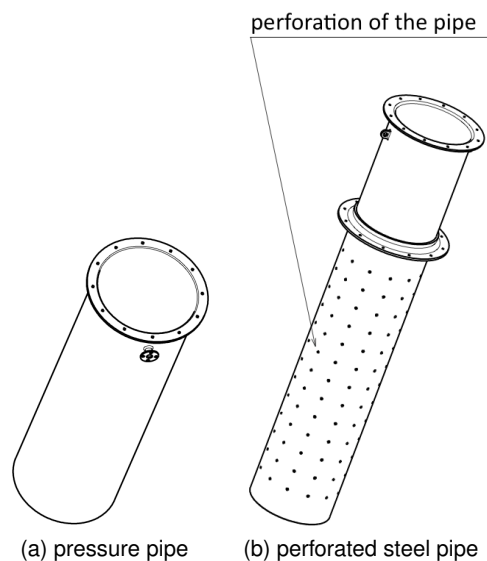


Figure 29: Details of the case of the second concept

Over a flange in the outer pipe a pump can be connected, as can be seen in figure 30. The pump introduces fluid into the gap between the two steel pipes. As the pressure increases, the fluid will start to travel through the perforation into the formation and finally into the completion. The fluid level in the borehole will then start to rise and, after some time, will reach the top of the simulator. An exit for the simulator is unavailable in this figure, but would be possible by attaching a valve on the cap. To monitor the pressure, a gauge will be placed on the sealed cap of the simulator.

Another advantage of the liquid throughput is related to the task of heating. The fluid can be preheated before it enters the pump, thereby allowing good controllability of the temperature. Measurements can be taken for the inflow and for the backflow; hence, reasonable results for temperature changes during the treatment can be achieved.

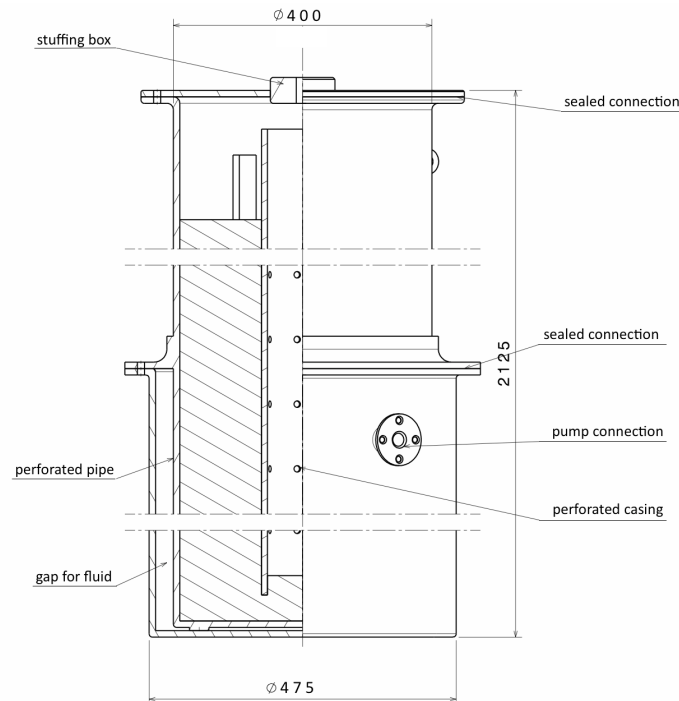


Figure 30: Cross-sectional view of the second concept

Figure 30 shows the cross section of the second concept of the simulator. Due to pressure, the simulator must be sealed. This is done at two spots: The first is located between the outer and the perforated pipe, while the second cap seals the borehole. To insert the ultrasonic transducer and the hydrophones, a stuffing box in the cap is needed to seal the cables that are required.

The dimensions of the simulator change slightly in contrast to the first concept. Therefore, although the dimensions of the frame would change to some extent, it would still be necessary to protect it from the risk of falling.

3.4 Laboratory Tests

3.4.1 Laboratory Test Device

For the laboratory measurements, a test device from Progress Ultrasonic AG was used (figure 31). This device is especially designed for test runs in the laboratory. It consists of three main parts: generator, casing and resonator.

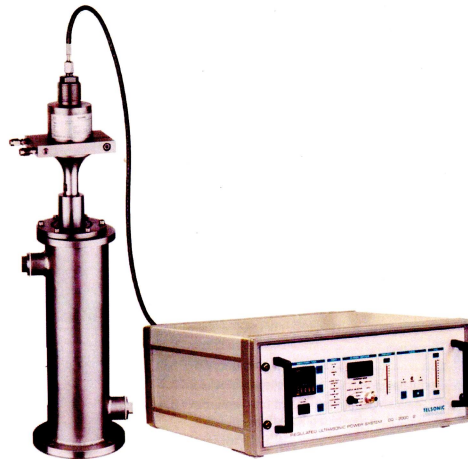


Figure 31: Ultrasonic generator

The generator has two operation modes. The first mode uses constant output power that can be set between 400 W and 2000 W , while the second one sends ultrasonic waves with a constant amplitude (can be varied between 50% and 100%). For the test, the second mode was used with an amplitude output of 100%.

The casing can be sealed and has two connections on the circumference. These allow a liquid throughput inside the casing. For the test runs, this casing was used inside a water bath with open connections to enable communication between the fluid of the water bath and that inside the casing.

In figure 32, the ultrasonic resonator is shown. It has an output power of 1000 W and produces ultrasonic waves with a frequency of 20 kHz . Due to generation of heat during the treatment, the resonator has two connections for cooling fluids, as visible on the left side of the figure.



Figure 32: Ultrasonic resonator

3.4.2 Test Runs at the University

The starting points of the test runs were the measurements carried out in the laboratory. These should provide an idea about attenuation and reflection of the produced ultrasonic waves. To get these measurements, ultrasonic treatments in a water bath with and without a casing were carried out. Thereby the a non-perforated and a perforated casing were used. First, a treatment with the resonator in the water bath was performed. No casing was used and an aluminum foil was inserted at a distance of 50 *cm* and 10 *cm* from the resonator, respectively. Aluminum is a rather soft material and the effects of the treatment become visible through erosion of the material. The test runs were planned to run for 10 minutes each.

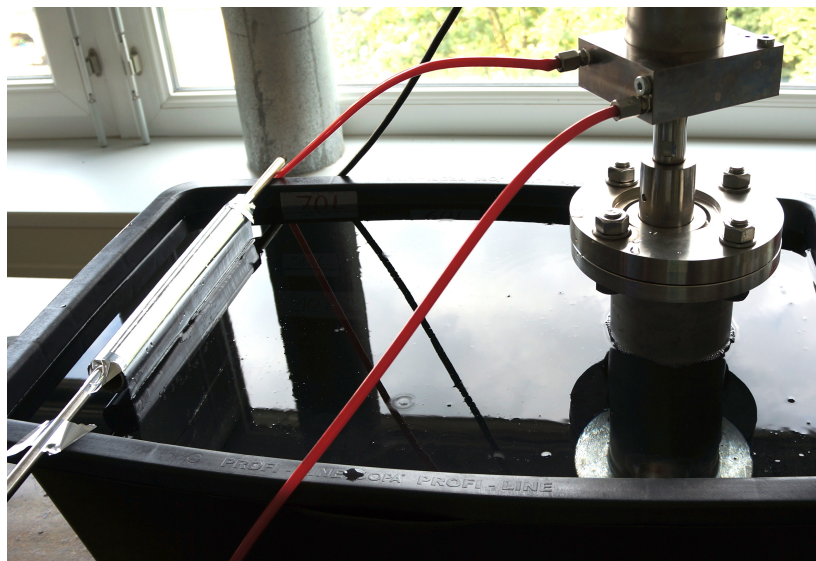


Figure 33: Test set-up for the ultrasonic treatment

In figure 33, the set-up of the laboratory test is displayed. On the right side, the ultrasonic resonator is inserted into a casing, whereas the aluminum foil is displayed on the left side of the picture.

Test runs 1 and 2

The first test run was performed without a casing with the foil at a distance of 45 *cm* from the resonator. After 10 *min*, the aluminum foil was visibly eroded (figure 34). The strongest effects could be detected at the edge of the foil. This was due to the reflection of the sonic waves from the wall of the container. An effect was also detected at the area of the foil that is perpendicular to the resonator. This can be explained by the angle of incidence. With an angle of zero, most of the sonic wave is transferred into the aluminum foil and only a small part is reflected.

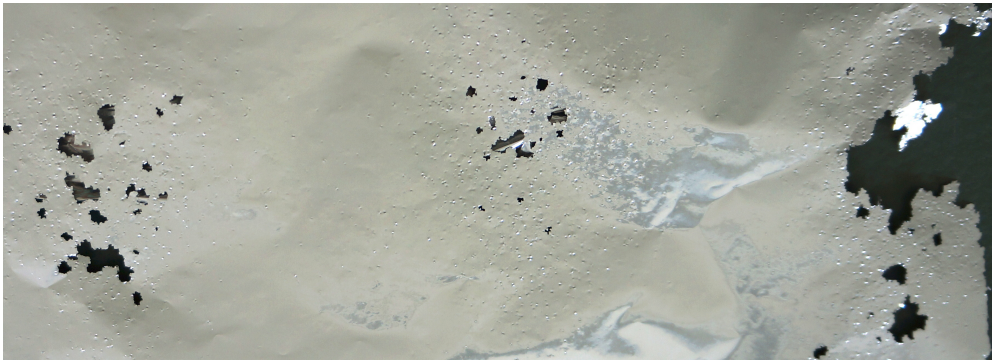


Figure 34: Ultrasonic treatment in a water bath 50 *cm* away from the resonator without a casing

The second one was carried out with a casing and the same distance of the foil to the resonator. It turned out that the casing shields held strong, with no visible effect being detected. For that reason, other runs were made with a smaller distance to the resonator.

Test runs 3 and 4

With a distance of 10 *cm* to the resonator, more visible effects were expected.

Figure 35a shows test 3 being performed without a casing. Immediately after starting the treatment, the first effects became visible. The test was then stopped after 2 *min* because the erosion happened too fast for the aluminum to withstand a 10 *min* run.

In contrast, the test with the casing showed a completely different result. As figure 35b shows, only a small impact was observed on the aluminum foil. The coins on the figures hint at the size of the erosion.

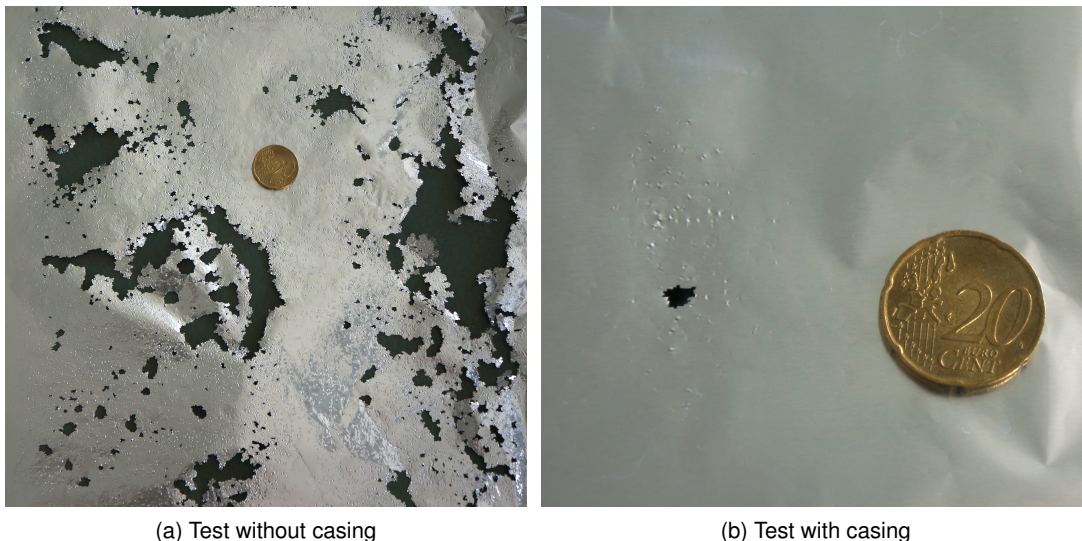


Figure 35: Ultrasonic treatment in a water bath 10 *cm* away from the resonator

Test runs 5 to 8

For comparison three test runs with a perforated casing at a distance of 10, 20 and 50 *cm* from the resonator were carried out with the perforations pointing at the aluminum foil (figure 36a). Furthermore, for the smallest distance an additional test run was done where the perforations do not exactly point to the aluminum foil (figure 36b).

The casing (figure 38b) has an outer diameter of 104 *mm* with 2 *mm* wall thickness and a length of 360 *mm*. The characteristics of the perforations are:

- 6 shots per foot
- 90° shot phasing
- 1/2" perforation diameter

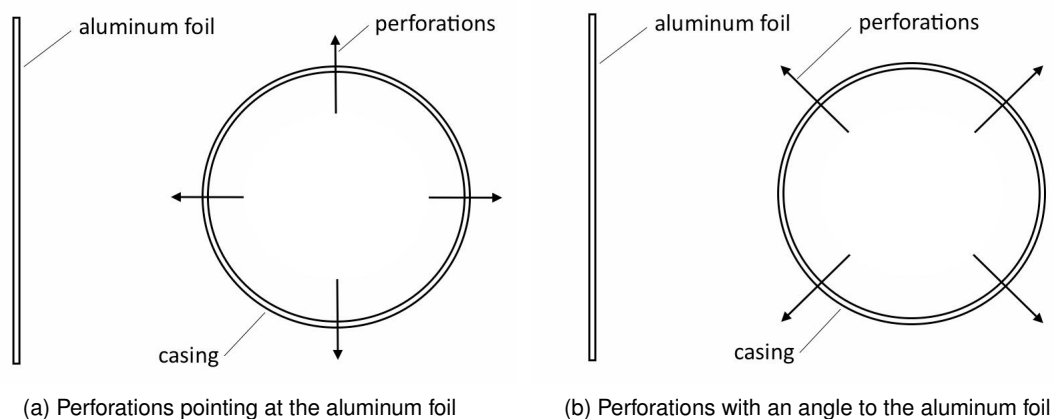


Figure 36: Test set up for the perforated casing

In figure 38a a perforated casing is described and in figure 38b the casing for the laboratory measurements is displayed.

The first run with a distance of 50 *cm* did not show any erosion marks after 10 *min*. In contrast to that, at a distance of 20 *cm* the aluminum foil was visibly eroded. However, this erosion was focused in the direction of the perforations (figure 37). The test run with a distance of 10 *cm* from the resonator (figure 39a) was, like for the tests without a casing, stopped after 2 *min*. In the direction of the perforations erosion started immediately at the beginning of the test. For the last run the casing was rotated for 45° (figure 36b). After 2 *min* the ultrasonic treatment showed visible effects. The erosion of the aluminum foil was more distributed and not as focused as for the last test (figure 39b compared to 39a). Due to the fact that no perforation was pointing at the foil, only the reflected and refracted waves caused erosion at the aluminum foil.

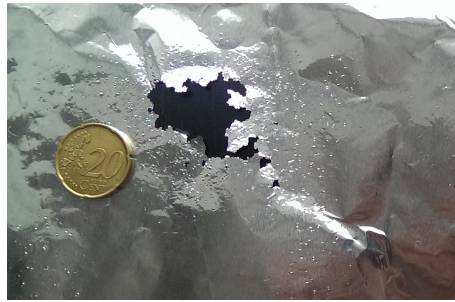


Figure 37: Test run with the perforated casing, perforations pointing at the aluminum foil at a distance of 20 *cm*

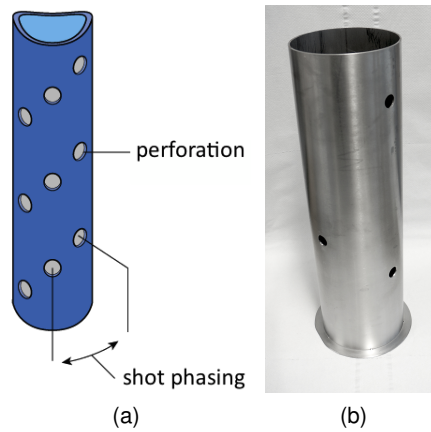


Figure 38: Example of a perforated casing and the casing for the laboratory tests



(a) Test, perforations directly pointing at the foil (b) Test, perforations with an angle to the foil

Figure 39: Ultrasonic tests in a water bath 10 *cm* away from the resonator with the perforated casing

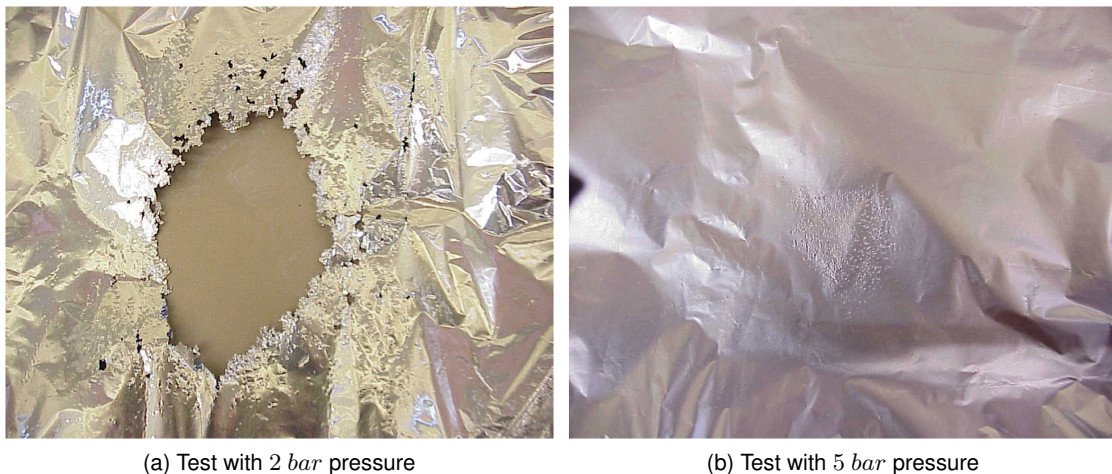
All tests up to that point have been performed under atmospheric pressure. In the next chapter, treatment with elevated pressure will be discussed.

3.4.3 Tests for Aquifer Cleaning

Ultrasonic treatment is also performed in terms of removing precipitations from water aquifers. This alteration of aquifers appears in many ways. However, in Germany, for example, the formation most often silts up (increasing amount of mud and sand which blocks the formation) or generates non-soluble encrustations, mostly from iron or manganese oxide (known as iron clogging), that block the formation. [31, p. 2]

Tests for the impact of ultrasonic treatment on these impurities were performed in the laboratory at the University of Mainz. However, these tests were carried out in a pressurized cell. Figure 40a shows the pressure being elevated to 2 *bar*. The used aluminum foil was strongly eroded and the typical noises of cavitation were recorded.

In contrast, the test run with a pressure of 5 *bar* showed different results (figure 40b): almost no erosion and the typical noise of cavitation was also missing. [31, p. 11]



(a) Test with 2 *bar* pressure

(b) Test with 5 *bar* pressure

Figure 40: Ultrasonic treatment for a water aquifer [31, p.11]

Thus, it is clear that the occurrence of cavitation strongly depends on the hydrostatic pressure. At atmospheric pressure, cavitation has the biggest influence, whereas up to a pressure of 5 *bar*, a strong reduction takes place. Above that pressure, the cavitation is negligible.

3.5 Final Simulator

The two raw concepts and the laboratory tests gave rise to new questions. Guided by the fact that the influence of cavitation decreases with increasing pressure, the focus of the simulator changed. From an initial focus on how the treatment behaves under various completions and fluids, the interest changed to the physical behavior of the ultrasonic treatment—e.g. what mechanism leads to the cleaning effect at elevated temperature and pressure conditions. This introduced some changes from the concepts to create a final simulator.

Originally, the simulator should have been capable of carrying out different completions but, in the end, only a casing was planned to run in the simulator. This casing should have the same characteristics as a casing used in the industry. However, it will be sealed with two caps to pressure up the insides of the casing. The first step of testing will run the ultrasonic resonator inside this casing with elevated pressure and temperature. In figure 41, only the first test run with the casing (red tube) is shown. The casing is mounted on a plate where a pump is connected via flow lines, as can be seen in the next figure. The cap has a stuffing box that seals the cables of the ultrasonic device, the hydrophones and the heating element.

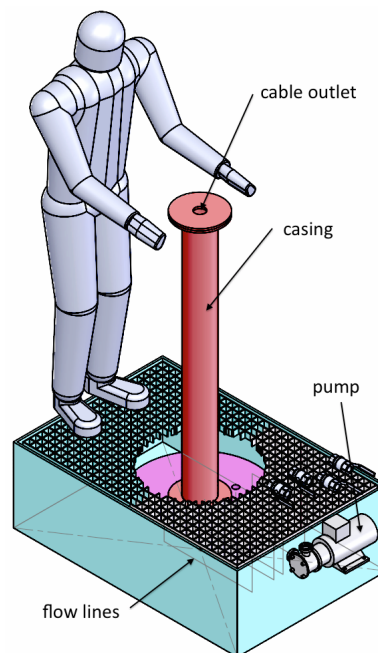


Figure 41: First simulation set-up of the final simulator with the casing only

Given pressures of a few hundred bar in a borehole and the fact that cavitation disappears at a fraction of it, this first simulation set-up should prove the mechanism of cleaning.

In figure 42, the second set-up for the simulation is constructed. Basically, it is the first set-up with an additional boiler. This boiler will also be filled with fluids and, in contrast to the first one, where the focus was on the cleaning mechanism, this set-up should give results for the attenuation through the casing. It will be possible to heat up and pressurize the casing. Further test runs are planned without a casing and with a perforated casing inside the boiler, respectively.

Since the boiler will be filled with different fluids that have to be disposed of, the whole simulator stands in a box (cyan box). It is designed in such a way that all fluids stored in the simulator during testing can be stored in the box in case of a leakage or if the fluids need to be disposed of.

From the first concept, the idea of using a cement sheet acting as a reservoir was canceled for the final simulator design. This will ease the manufacturing, but the idea has been kept in mind for later designs.

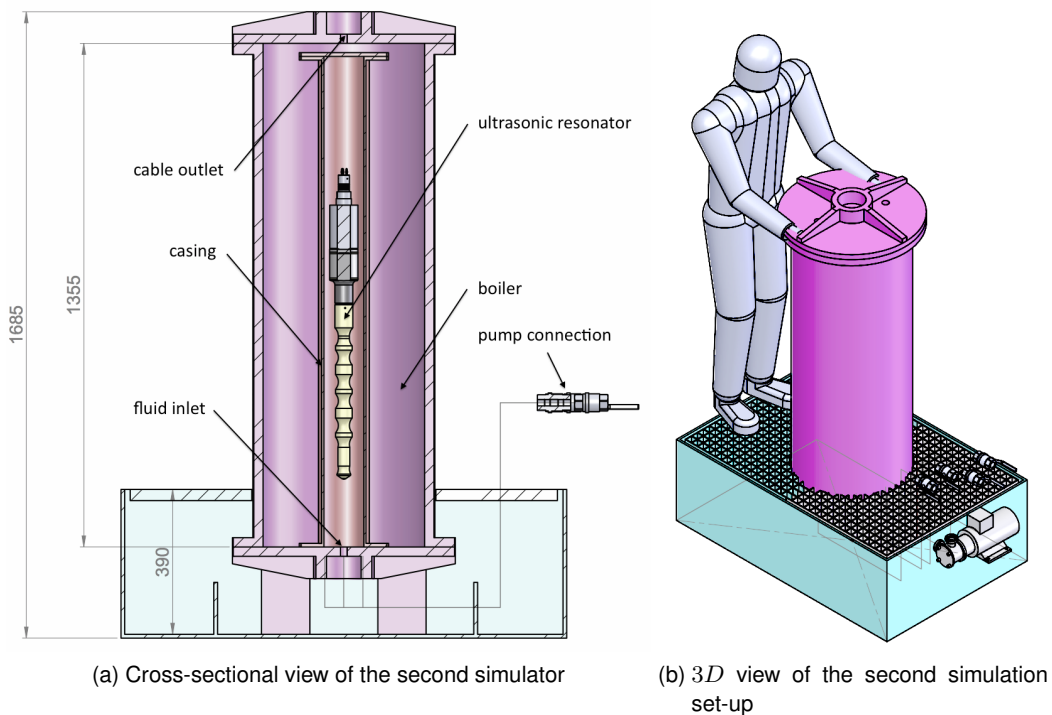


Figure 42: Second simulation set-up with the casing and the boiler

At the bottom of figure 42a, the black lines indicate the flow lines. With them, the simulator can be filled, emptied or circulated.

To gain reasonable results from the ultrasonic testing, the reflection of the ultrasonic waves from the boiler wall must be minimized, which will be done using insulating material. It will cover the boiler wall on the inside and lead the ultrasonic waves to subside. This arrangement is called acoustic swamp and it is absolutely necessary for achieving reasonable results.

3.6 Cost Estimation

The last section focuses on an economical estimation of the simulator. The realization of the simulator will be done in the near future and this part should be a guideline how much money must be spent on parts and material. Even, if expensive parts like hydrophones are needed, costs can increase rapidly and the whole simulator can become uneconomic. For example, the range of the hydrophones starts from a few hundred euro for a simple hydrophone with earphones and batteries, up to nearly 50,000€ for a fiber optical hydrophone. Therefore, this is the most critical part of this estimation. To measure attenuation more than one hydrophone must be used. Ideal would be at least an array of 6 hydrophones placed at different distances from the resonator and the casing, respectively. However, this would be major a cost driver.

The cost estimation does strongly depend on the pressure for which the simulator is planned to run. Single parts like valves or sensors do strongly increase which increasing pressure capability. For this first cost estimation a maximum pressure of 20 *bar* was chosen. In table 2 all necessary parts are listed and a rough estimation has been done.

Table 2: Price list of the parts of the simulator

Part	Price/Unit [€/#]	Units [#]	Price [€]
Hydrophone + accessories	550	6	3300
Underwater Sound Recording, Notebook Computer	1,370	1	1,370
Blow-off valve	19	1	19
Manometer	22	1	22
Check valve	46	2	92
Ball valve	26	5	130
Screw-in temperature sensor	14	1	14
Centrifugal pump	310	1	310
Pressure sensor	138	1	138
Simulator frame			
Pressure chamber, welded for 20 <i>bar</i> with 2 cover, screwed			9,048
Conservation, sandblasted, prime coated and painted			368
Container 1200/800/390 <i>mm</i> with grid			688
Sum			15,499
Price incl. taxes			18,599

All prices were requested from different companies and can be seen in the appendix.

The other part of the simulator is the frame and can be constructed in a metal working shop. Their offer is also enclosed in the appendix. Finally, the whole simulator would cost approximately 19,000€ (including tax).

4 Results/Conclusion

Even after decades of studies and tests, the phenomenon of ultrasonics is still not fully understood. High non-linearities and difficult treatment set-ups are key points that complicate the concept. One important accompanying effect of ultrasonic waves in fluids is the occurrence of cavitation. However, this process strongly depends on the surrounding conditions, especially on the pressure. This study on ultrasonic behavior showed that the main process of cleaning at atmospheric pressure strongly decreases at elevated pressure. The performed laboratory tests at atmospheric pressure indicated evidence of cavitation. The characteristic noise and strong erosion were recorded at all test runs at atmospheric pressure. Test runs with the ultrasonic tool (with 20 kHz) in a water bath without a casing proved that the effect of cavitation is still strong, even at a distance of nearly half a meter away from the resonator. However, as steel casings were implemented for the test runs (perforated and non perforated), it was observed that the steel body of the casing almost completely dampens the ultrasonic waves. In the tests with the ultrasonic resonator in the center of the casing, at a distance of 5 cm behind the casing wall, nearly no erosion due to cavitation was visible for the run with a non perforated casing. However, the test runs with the perforated casing showed, that the erosion is still very high, although the perforations have only a diameter of $1/2''$.

Tests performed at the University of Mainz refuted the existence of cavitation at pressures above 20 bar . [31] Even at 5 bar , the influence of cavitation on the cleaning process decreases considerably. Therefore, the treatments reveal which effects are responsible for the cleaning mechanism at elevated hydrostatic pressure to improve the treatment in the field and increase the success rate.

Based on that information, the first two drafts of the simulator, developed at the beginning of the project, were changed. The initial focus was on determining how ultrasonics influence the near wellbore area, the cement sheath and the perforations. This focus then shifted to the investigation of physical processes during the ultrasonic treatment in the fluid. In particular, the influence of pressure and temperature on the cleaning effect. Therefore, the final simulator, which is designed based on these findings, will be capable of handling elevated pressures and temperatures. This is principally a pipe-shaped pressure chamber, standing in a box with flow lines connected to a fluid pump that allows the change of fluids. In combination with the use of hydrophones during the treatments a better understanding can be expected. This is necessary for improving the ultrasonic cleaning, which could become an alternative to chemical treatments. Besides saving costs, the more important fact is the environmental aspect. This treatment will reduce the amount of chemicals used for well treatments, a key target, especially in countries where this is still not a big issue. Furthermore, the construction of this simulator was calculated and would cost approximately $19,000\text{€}$ (including tax).

5 Appendices

Thru-hole/Hull Mounted Hydrophone and Receiving Array



BII-7017 Type 5, 26dB gain Preamplifier +custom HP filter, 6" wires, Wire Leads, 300m depth rating, \$756.60

BII-7017 Thru-hole/Hull Mounted Hydrophone: Hull Mounted Receiving Array

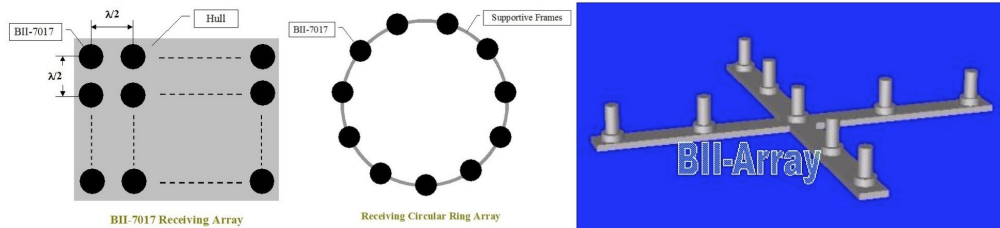
A BII-7017 hydrophone is designed to be mounted on the wall/hull of underwater submersibles, pipes, tanks and vessels to detect the acoustic signals outside a submersible or inside a pipe, tank or vessel. Hull mounted receiving array (such as linear, planar and cylindrical array) can be configured easily with BII-7017 hydrophones. With built-in preamplifiers and custom high pass filters, the array can drive long cables and eliminate the unwanted ship or ambient noise before beam-steering and amplitude shading. Depending on the operating frequency, these hydrophones can be treated as Point, Line or Rectangle Aperture element in array signal processing.

Bearing of sound source can be estimated by maneuvering the supportive fixture to minimize the difference in signal level between the two BII-7017 hydrophones. Moving object (AUV/UUV/ROV, tagged marine animal, underwater robot, etc.) can be tracked with short-baseline or ultra-short-baseline consisting of BII-7017 receivers.

For thru-hole mounted spherical hydrophone, please click [BII-7000 Broadband Omnidirectional Hydrophone](#).

For thru-hole mounted conical beam planar hydrophone, please click [BII-7070 Directional Planar Hydrophone](#).

For a towed array, fixed array and drifting array, you may consider [BII-7030 Bolt Fastening Hydrophone](#).



Suggested Application

Hull Mounted Receiving Array
 Point, Line or Rectangle Aperture element in array signal processing
 Underwater Vehicles: AUV/UUVs and ROVs
 Long-baseline, Short-baseline, Ultra-short-baseline Positioning
 Measurement of Target Bearing, Direction-finding Sonar System
 Tracking of Pingers/Acoustic Tags/Transmitters
 Locating Marker, Pinger, Beacon and Positioning Devices Underwater
 Hydrophone Array in Multibeam Sonar System
 Underwater Equipment, Instruments and Submersibles
 Acoustic Pressure Sensors inside Pipe, Tank and Vessel

General Purpose Low Noise Hydrophone
 Noise Monitoring
 Sonobuoy
 Low Power Acoustic Projector
 Natural, Anthropogenic and Bioacoustic Underwater Sounds
 Hydrophone Array and Passive SONAR
 Bioacoustic Research
 Field Studies of Marine Animals (Fishes, Whales and Dolphins)
 Passive Acoustic Monitoring (PAM System)
 Underwater Sound Recording and Listening

Figure 43: Data sheet for hydrophone

Underwater Sound Recording, Analysis, Synthesis & Playback

Notebook Computer Windows 8
 15.6" LCD display
 250 GB HDD
 1 GB Memory
 Real-Time, Recording, Post-Process
\$1866



BII-7530, BII-7032, BII-8005 play and record underwater sounds in water tank at BII.

The BII-8005 is a portable and advanced sound recorder and synthesizer with the latest laptop technology. It records, analyzes and playbacks sounds, and synthesizes Sonar signals for underwater acoustic systems (Active SONAR, communication, beaconing ...).

With BII-8005s transmitting and receiving sounds, field experiments of your ideas and acoustic devices are easy and convenient, it speeds up the tryout and commissioning of your equipment and algorithm by tuning parameters on virtual instrument panel of BII-8005.

Typical signals BII-8005s generate and analyze include Pulsed SINE, Chirp/FM, FSK, natural sounds and marine animal sounds, the signal is processed in time, frequency and time-frequency domain. You may utilize these powerful tools to investigate the signals in detail and to commission the acoustic systems in fields such as noise measurement, bioacoustics, FSK digital communication, echo sounding, sub-bottom profiling, beaconing...

With BII-8005, you may speed up your filed project on following subjects:

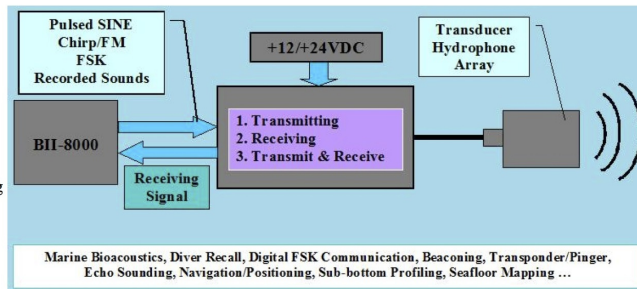


Figure 44: Data sheet for recording and analysing unit

**Sicherheitsmanometer NG63,****60,50 EUR**zzgl. 19 % USt zzgl. [Versandkosten](#)

Lieferzeit 3-4 Wochen

Gewicht: 0,20 KG

Unser Typ: SN63

 Produktbeschreibung

- ◆ Rohrfedermanometer S3 gemäß EN 837-1
- ◆ Mit bruchsicherer Trennwand und ausblasbarer Rückwand
- ◆ Größe: Ø63mm
- ◆ Genauigkeitsklasse: 1,6%
- ◆ Messsystem: Edelstahl 1.4571
- ◆ Gehäuse: Bajonettring-Gehäuse, Edelstahl
- ◆ Scheibe: Sicherheitsverbundglas

Sicherheitsausführung S3 nach EN 837-1, mit bruchsicherer Trennwand aus Edelstahl 1.4301 zwischen Messsystem und Zifferblatt sowie ausblasbarer Rückwand; bei Druckaufbau im Gehäuse wird der gesamte Querschnitt nach hinten freigegeben.

Flüssige oder gasförmige Messstoffe (im Rahmen der Beständigkeit der Messstoffberührenden Teile), nicht hochviskos und nicht kristallisierend, in Umgebungen, wo ein besonders dichtes, chemisch widerstandsfähiges Gehäuse benötigt wird (z.B. Freianlagen, Nassbetriebe, aggressive Atmosphäre) und es auf erhöhte Sicherheit für den Betrachter ankommt.

Figure 45: Data sheet for manometer



Weitere Produktbilder



VERGRÖßERN

Sicherheitsventil - MS - Druckluft - 0,25-50bar DN8 Baumustergeprüft

Art. Nr.: 855811100020

ab **€ 15,14**

\$ 20.76

inkl. MwSt. € 18,02

\$ 24.71

zuzügl. Versandkosten

★★★★★ (2)

Kurzbeschreibung

- Sicherheitsventil als druckentlastende Sicherheitseinrichtung für druckbeaufschlagte Räume (z.B. Dampfkessel, Druckbehälter, Rohrleitungen)
- Für Druckluft und andere ungiftige, nicht brennbare Gase, frei abblasend

mehr...

» [Fragen zu diesem Artikel?](#)

» [PDF-Prospektblatt](#)

» [Artikel merken](#)

» [Artikel weiterempfehlen](#)

» [Lesezeichen setzen](#)

Angebot anfordern

Detailbeschreibung	Ausführung	Versandkosten	Video	PDF	Bewertungen
--------------------	------------	---------------	-------	-----	-------------

Ausführung

Ansprechdruck	Gewinde	Abblaseleistung
(alle anzeigen) 0,27 bar 0,3 bar 0,4 bar 0,5 bar	(alle anzeigen) G 1/2" G 1/4" G 3/8"	(alle anzeigen) 500 m³/h

[Alle Filter zurücksetzen](#)

	Ansprechdruck	Gewinde	Abblaseleistung	Preis	inkl. MwSt.	Art. Nr.
<input type="checkbox"/> x	20 bar	G 1/4"	500 m³/h	€ 15,43 \$ 21.16	€ 18,36 \$ 25.18	855811120022
<input type="checkbox"/> x	20 bar	G 3/8"	500 m³/h	€ 15,14 \$ 20.76	€ 18,02 \$ 24.71	855811120023
<input type="checkbox"/> x	20 bar	G 1/2"	500 m³/h	€ 16,14 \$ 22.14	€ 19,21 \$ 26.34	855811120024

Figure 46: Data sheet for safety valve

JUMO Mess- und Regelgeräte GmbH

Pfarrgasse 48 Tel.: +43 1 61061-0 E-Mail: info@jumo.at
 1230 Wien, Austria Fax: +43 1 61061-40 Internet: www.jumo.at



More than **sensors + automation**

Angebot Nr. 160494

JUMO Mess- und Regelgeräte GmbH, 1230 Wien, Austria

Montanuniversität Leoben
 Peter-Tunner-Str. 27
 8700 Leoben

Datum 02.06.2014
 Ihre Kunden Nr. 10059

Seite 1 von 2

Für Ihre Rückfragen

Jürgen Spörk
 Tel.: 0043 1 61061 18
 Fax: 0043 1 61061 40
 Mail: Juergen.Spoerk@jumo.net

Unser Außendienst für Sie

Anton Pausackl
 Tel.: 00431610610
 Fax: 004316106140
 Mail: anton.pausackl@jumo.net

Ihre Anfrage
Anfragedatum: 02.06.2014

Pos.	Beschreibung	Menge Einheit	Einzelpreis	Positionswert
1	JUMO Teile-Nr.: 00546123 Bestellschlüssel: 401002/000-461-405-502-20-601-61/000	1 Stk	162,46 EUR -15 % Rabatt 15%	
			138,09 EUR	138,09 EUR

Druckmessumformer
 JUMO MIDAS C08

Typ	JUMO MIDAS C08
Eingang	0..25 bar Relativdruck
Ausgang	4..20mA zI
Prozessanschluss	G 1/4 DIN EN 837
Wst.Prozessanschluss	CrNi (Edelstahl)
Dichtung	FPM
Elektr.Anschl.Art	Leitungsdose DIN EN 175301-803, Form A
Nenngr. Druckanschl.	G1/4
Messbereichs-Anfang	0
Messbereichs-Ende	25
Messbereichs-Einheit	bar
Spannungsversorgung	DC8...30V
Firmenzeichen	JUMO- Logo



Das obige Bild stellt ein Beispielbild aus der Produktgruppenfamilie dar.


Lieferzeit Ab Lager, solange der Vorrat reicht


Handelsgericht: Wien, Firmenbuchnummer: 124393 g, DVR Nr.: 0143791, UID Nr.: ATU15069903, ARA Lizenz Nr.: 268-AS 18313132
 Bankverbindung: BA-CAAG, BLZ 11000, Konto: 0046-36320/00, IBAN-Code: AT70 1100 0004 6363 2000 BIC: BKAUATWW

Figure 47: Data sheet for pressure sensor

Einschraubfühler mit M8x50 Gewinde bis 105°C

24





Sofort lieferbar.

F Empfehlen

+1

i

F Empfehlen

+1

i

F Empfehlen

+1

i

ZOOM

letzt drucken
empfehlen


Sensor:	Bitte wählen Sie:	↕
Leitungslänge:	erst Sensor wählen	↕
Schaltungsart:	erst Leitungslänge wählen	↕

ab 13.50 €

Figure 48: Data sheet for screw-in temperature sensor


Kugelhähne & Sicherheitsarmaturen

» Home » Produkte » Durchgangskugelhähne mit Gewindeanschluss » Messingkugelhahn 998



998 **Kugelhahn aus Messing**

- Kugelhahn aus Messing
- Voller Durchgang
- Beidseitig Innengewinde nach DIN ISO 228
- Hebelgriff (rot)
- Kennzeichnung nach DIN EN 19
- Ausblässichere Schaltspindel mit doppelter O-Ring Abdichtung
- Sicherheitsbewusste Spindel dimensionierung mit Stahlgriff
- Die Festigkeitsanforderungen der drucktragenden Gehäuseteile sind nach DIN EN 331 ausgelegt
- (VE = Verpackungseinheit)

 [Datenblatt](#)

Größe	DN	Druck bar	Länge mm	Gewicht kg	Preis * €/St.	VE
1/4"	6	25	41,5	0,140	3,35	10
3/8"	10	25	41,5	0,120	3,35	10
1/2"	15	25	51	0,220	5,20	10
3/4"	20	25	54	0,320	7,45	8
1"	25	25	67	0,495	11,45	5
1¼"	32	25	77	0,775	18,00	3
1½"	40	25	90	1,035	25,40	2
2"	50	25	106	1,570	36,85	2

* Lieferung nur an Industrie, Handel und Gewerbe · Alle Preise zzgl. gesetzl. MwSt. plus Versandkosten
[Home](#) | [Produkte](#) | [Kontakt](#) | [Aktuelles](#) | [Unternehmen](#) | [Rechtliches](#) | [Download](#) | [Datenschutz](#)
 G. Bee GmbH · Robert-Bosch-Straße 14 · 71691 Freiberg · Germany

Figure 49: Data sheet for ball valve



MS - HORIZONTAL SINGLE STAGE CENTRIFUGAL PUMP

Applications: Cooling water, Domestic water supply, Sprinkler systems, Agriculture, Boosting & circulation systems, Water treatment

Performance range:

Capacity: Q up to 27 m3/h
 Head: H up to 28m
 Max operation pressure: 8bar
 Liquid temperature: -10°C to 85°C
 Speed: n2900rpm
 Power: P up to 2.2kw



Standard material: All the parts contact with liquid made of 304 stainless steel. Carbon/Silicon Carbide mechanical seal as standard.

Description: Hydraulic parts. All stainless steel horizontal single stage not self-priming pump with axial suction, vertical discharge threaded connections.

MS					
PART No.	Q (max) m3/hr	H (max) m	P2 (shaft power) kW	n rev/min	LIST (ex GST)
CNP-MS60/0.37M	4.8	18	0.37 KW 1PH	2900	\$412
CNP-MS60/0.37T	4.8	18	0.37 KW 3PH	2900	\$340
CNP-MS60/0.55M	4.8	23	0.55 KW 1PH	2900	\$442
CNP-MS60/0.55T	4.8	23	0.55 KW 3PH	2900	\$370
CNP-MS60/0.75M	4.8	28	0.75 KW 1PH	2900	\$539
CNP-MS60/0.75T	4.8	28	0.75 KW 3PH	2900	\$456
CNP-MS100/0.55M	8.4	18	0.55 KW 1PH	2900	\$436
CNP-MS100/0.55T	8.4	18	0.55 KW 3PH	2900	\$364
CNP-MS100/1.1M	9.6	27	1.1 KW 1PH	2900	\$635
CNP-MS100/1.1T	9.6	27	1.1 KW 3PH	2900	\$533
CNP-MS160/0.75M	12	15	0.75 KW 1PH	2900	\$538
CNP-MS160/0.75T	12	15	0.75 KW 3PH	2900	\$453
CNP-MS160/1.1M	12	20	1.1 KW 1PH	2900	\$639
CNP-MS160/1.1T	12	20	1.1 KW 3PH	2900	\$536

Figure 50: Data sheet for pump

The chosen pump has a maximum operating pressure of 8 bar, which is not enough to pressure up the simulator to operating conditions. There would be the possibility to take a pump, which is capable for 20 bar. However, pumps with this requirements are much more expensive. A cheaper solution would be to fill the simulator with fluid, seal up and connect a high pressure cleaner to get the 20 bar pressure.



Grazer Vorstadt 120a
 A-8570 Voitsberg - Austria
 Tel 03142 - 25 5 90
 Fax 03142 - 25 5 90 -4
 Mail: metallbau.schuster@aon.at
 ATU 30403809 FN 6086 K

Bernd Strommer

8564 Ligist

Angebot: 2140494

Datum 02.06.2014
 Kunden Nummer 0
 Unsere UID-Nr. ATU 30403809

Anfrage: Bohrlochsimulator

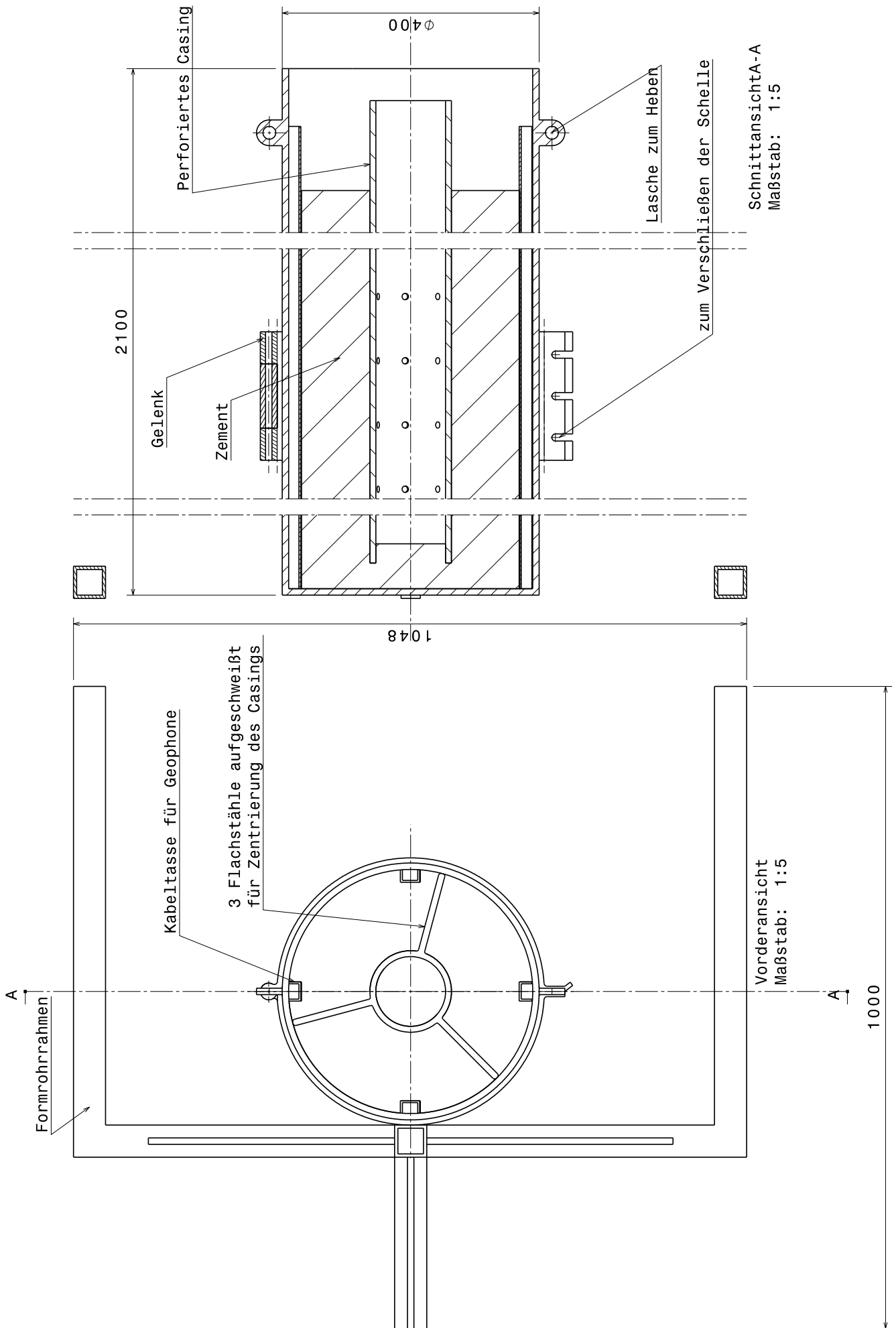
Wir danken für die Anfrage und freuen uns, Ihnen die angefragten Positionen gemäss unseren allgemeinen Geschäftsbedingungen, freibleibend anzubieten:

POSITION	ARTIKEL	EINZELPREIS	GESAMTPREIS
1	Stahlbau - Druckbehälter mit 2 Deckel geschraubt Innenteil eingepaßt lt. Zeichnung Maße : dm440x 1355mm Material , Schweißverfahren und Druckbereich nach genauer Spezifikation und Vorgabe. 1 Stk.	9.048,00	9.048,00
2	Konservierung - lt. Vorgabe Sandstrahlen,grundieren und mit Decklack lt. RAL.... lackiert 1 Stk	368,00	368,00
3	Stahlbau - Unterbau mit Aufnahme 1200/800/390mm Wanne mit Gitterrost 1 Stk.	688,00	688,00
Summe			10.104,00
zuzüglich 20,00% Mwst			2.020,80
Angebotssumme €			12.124,80

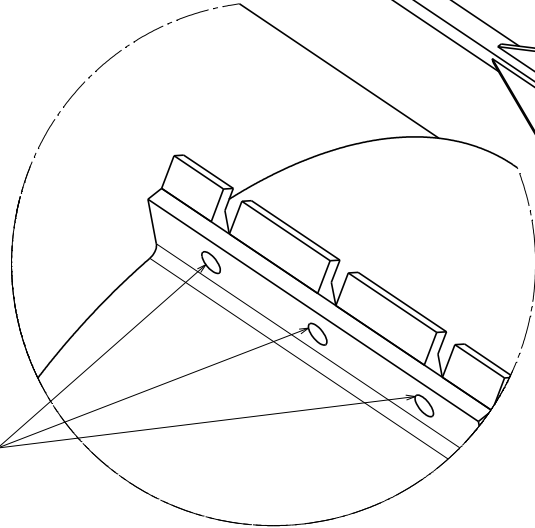
Zahlungskondition *Teilzahlung n. Vereinbarung bei Fertigstellung Rest*
 Zahlart *BIC/RZSTAT2G487 IBAN/AT 543848 7000 00030114*
 Lieferkondition *Lieferung nach Vereinbarung und techn.Klarheit*
 Versandart *Abholung*

Wir hoffen unser Angebot entspricht Ihren Vorstellungen. Für eventuelle Rückfragen stehen wir Ihnen selbstverständlich gerne zur Verfügung. Ausschließlicher Gerichtsstand ist A-8570 Voitsberg. Die Ware bleibt auch bei Weiterveräußerung bis zur vollständigen Bezahlung unser Eigentum.

Figure 51: Offer for the frame

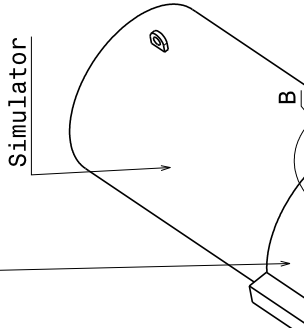


Verschließen mittels 3
Schraubenverbindungen



Detail B
Maßstab: 1:2

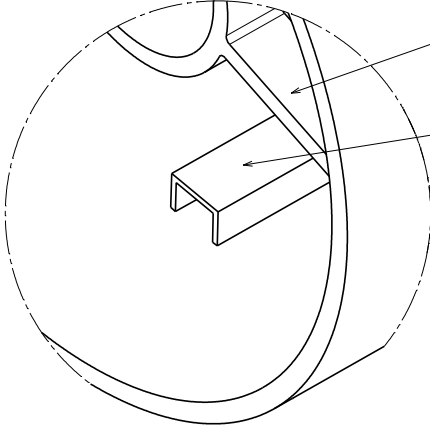
Stütze für Simulator



Simulator

A

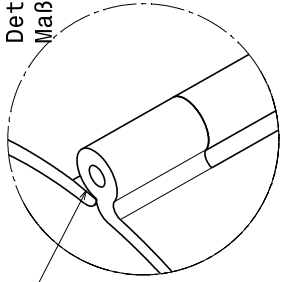
Detail C
Maßstab: 1:2



Kabeltasse für Geophone

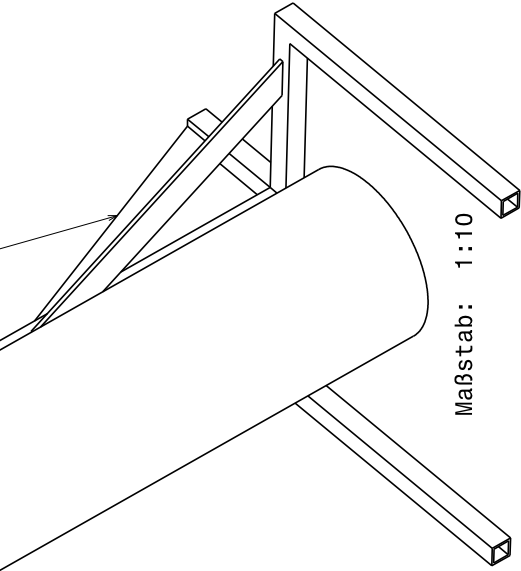
3 Flachstähle zur
Zentrierung des Casings

2-teilige Schelle mittels Bolzen
gelagert zum Öffnen/Schließen



Detail A
Maßstab: 1:2

Verstrebungen für Formrohre

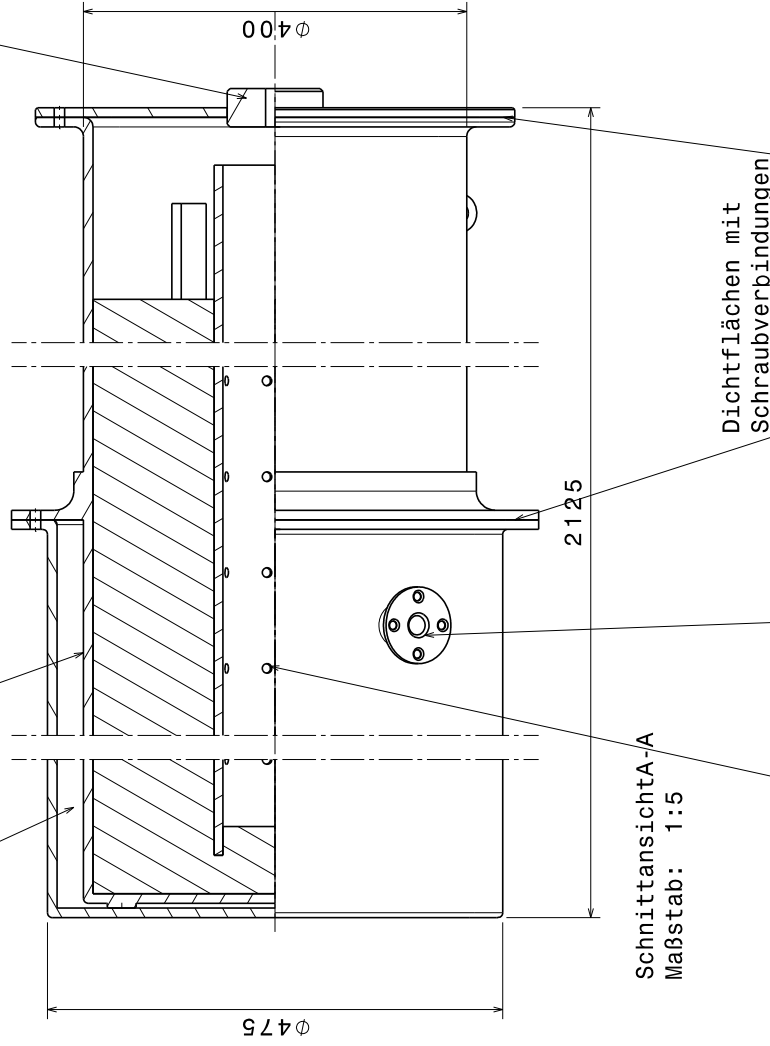
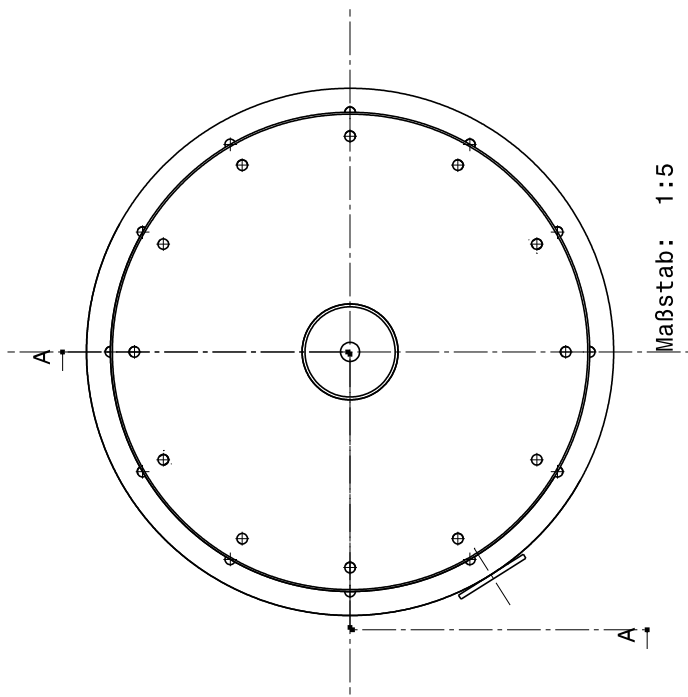


Maßstab: 1:10

Maßstab: 1:10

Flüssigkeitskammer
Deckel mit Stopfbüchse
zum Abdichten der Kabel

Flüssigkeit über perforiertes
Außenrohr in den Zement geleitet

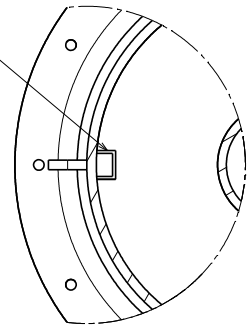


Schnittansicht A-A
Maßstab: 1:5

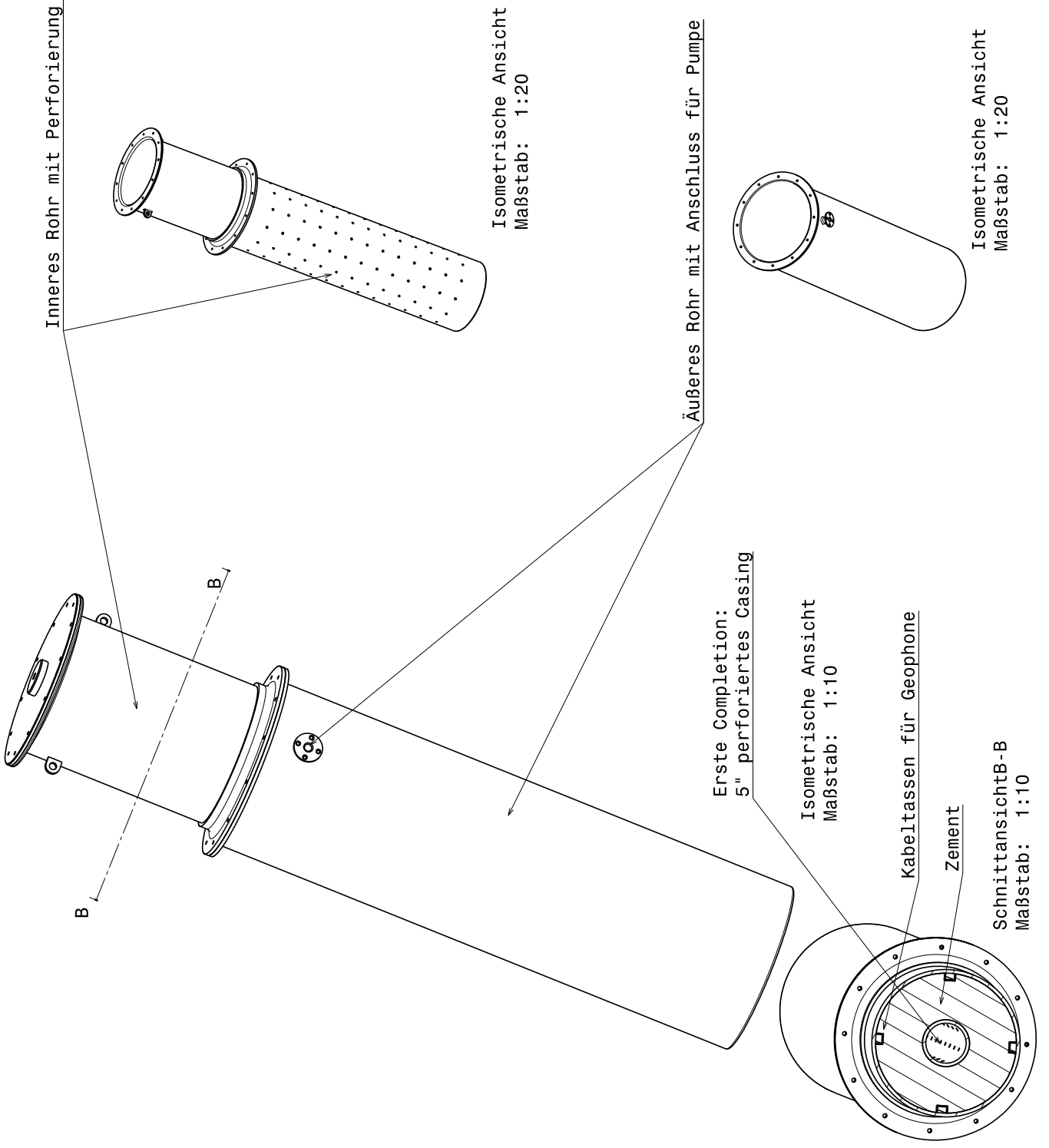
Dichtflächen mit
Schraubverbindungen

Anschluss für Pumpe

Kabeltassen für Geophone



Flüssigkeit fließt dann durch den
Zement in das perforierte Casing



Inneres Rohr mit Perforierung

Isometrische Ansicht
Maßstab: 1:20

Äußeres Rohr mit Anschluss für Pumpe

Isometrische Ansicht
Maßstab: 1:20

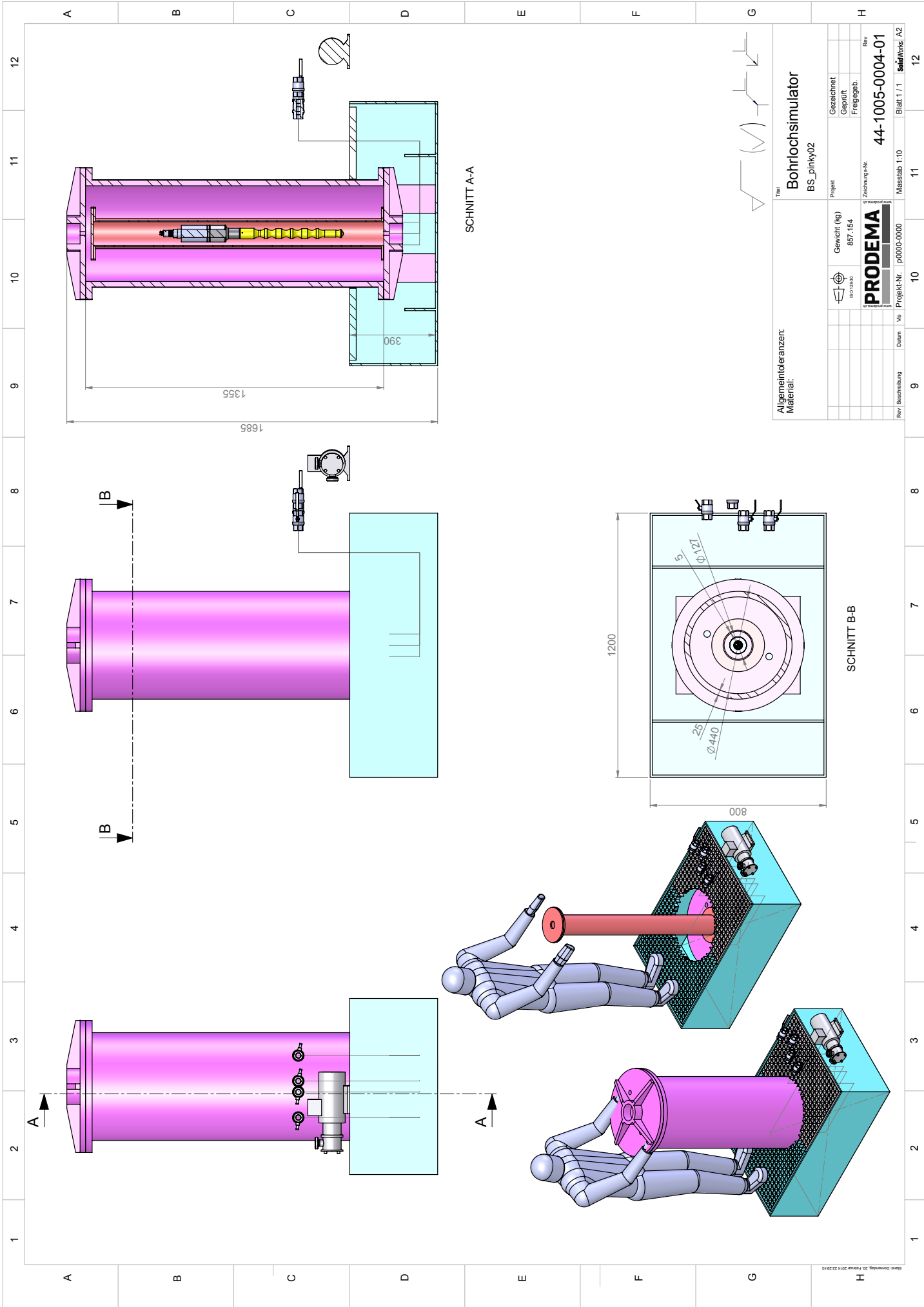
Erste Completion:
5" perforiertes Casing

Isometrische Ansicht
Maßstab: 1:10

Kabeltassen für Geophone

Zement

Schnittansicht B-B
Maßstab: 1:10



Teil: Bohrlochsimulator
BS_pinky02

Projekt	Gezeichnet	Geprüft	Freigegeben	Rev
Gewicht (kg)	857,154			
PRODEMA				
Projekt-Nr.	44-1005-0004-01			
Rev				
Rev	Bearbeitung	Datum	Von	Projekt-Nr.
				p0000-0000
				Blatt 1 / 1
				ScaleWorks A2
				12

Algemeintoleranzen:
Material:

References

- [1] R. J. Saucier, "Considerations in gravel pack design," tech. rep., Society of Petroleum Engineers, 1974.
- [2] M. F. Hamid and W. R. W. Sulaiman, *Fundamentals of Petroleum Engineering - Well Completion and Stimulation*.
- [3] J. D. Clegg, *Petroleum Engineering Handbook, Volume IV: Production Operations Engineering*. Society of Petroleum, 2007.
- [4] Petroleum Support. (undated). Open Hole. [Online]. Viewed 2013 November 21. Available: <http://petroleumsupport.com/well-completion-method/open-hole/>.
- [5] M. Crabtree *et al.*, *Fighting Scale - Removal and Prevention*, 1999.
- [6] J. Outlaw, "Differential scanning calorimetry," tech. rep., PerkinElmer, Inc., 940 Winter Street, Waltham, MA02451 USA, 2011.
- [7] J. Ring *et al.*, "Simulation of paraffin deposition in reservoirs," tech. rep., SPE Production and Facilities, 1994.
- [8] Halliburton, "Production enhancement-paraffin and asphaltene control." PDF File, 2005.
- [9] K. J. Leontaritis, "Case study of a successful wax diagnosis an intervention," *Oil and Gas Journal*, 1998.
- [10] Flow Assurance. (undated). PVT. [Online] Viewed 2013 December 5. Available: <http://flowassurance.blog.com/flow-assurance-topics/>.
- [11] Jamaluddin *et al.*, "Laboratory techniques to measure thermodynamic asphaltene instability," *Journal of Canadian Petroleum Technology*, 2002.
- [12] M. Trbovich and G. King, "Asphaltenen deposit removal: Long-lasting treatment with a co-solvent," tech. rep., Society of Petroleum Engineering, Inc., 1991.
- [13] GOTCO International. (undated). Remedial and Repair - Casing Scraper. [Online]. Viewed 2014 May 26. Available: <http://www.gotco-usa.com/pdf/casingscraper.pdf>.
- [14] Girard Industries. (undated). Tremco Pipeline Equipment. [Online]. Viewed 2014 June 6. Available: <http://www.tremcopipeline.com.au/pdf/girard/girard-brochure.pdf>.
- [15] D. B. Bennion and F. B. Thomas, "Formation damage due to mineral alteration and wettability changes during hot water and steam injection in clay-bearing sandstone reservoirs," tech. rep., Hycal Energy Research Laboratories, 1992.

- [16] Montana State University. (undated). Paraffin Asphaltene Removal and Control. [Online]. Viewed 2013 November 20. Available: <http://www.parc400.com/removal.htm>.
- [17] H. Kuttruff, *Physik und Technik des Ultraschalls*. S. Hirzel Verlag Stuttgart, 1988.
- [18] University of Washington. (undated). Ultrasonic. [Online]. Viewed 2013 November 20. Available: <http://courses.washington.edu/bioen508/Lecture6-US.pdf>.
- [19] Brookly College. (undated). Earthquakes. [Online]. Viewed 2014 January 10. Available: <http://academic.brooklyn.cuny.edu/geology/grocha/plates/platetec18.htm>.
- [20] Wordpress. (undated). The Piezoelectric Effect in Quarz. [Online]. Viewed 2014 January 10. Available: <http://taobabe.wordpress.com/the-body-piezo-electric>.
- [21] R. Lerch *et al.*, *Technische Akustik - Grundlagen und Anwendungen*. Springer, 2009.
- [22] J. Krautkrämer and H. Krautkrämer, *Ultrasonic Testing of Materials*. Springer, 1990.
- [23] Montana State University. (undated). Piezoelectric Polymers. [Online]. Viewed 2014 January 10. Available: <http://www.physics.montana.edu/eam/polymers/piezopoly.htm>.
- [24] Armadawater (undated). High Sheer Reactor. [Online]. Viewed 2014 January 14. Available <http://www.armadawater.com/innovation/high-sheer-reactor/>.
- [25] C. H. Sherman and J. L. Butler, *Transducers and Arrays for Underwater Sound*. Springer Science and Business Media, 2007.
- [26] J. L. Delany, "Bender transducer design and operation," tech. rep., Ultra Electronics Ltd, Sonar and Communication Systems, 2000.
- [27] S. Goodman *et al.*, "Field demonstration of a dfb fibre laser hydrophone seabed array in jervis bay, australia," tech. rep., Defence Science and Technology Organisation, 2009.
- [28] S. Foster *et al.*, "A fibre laser hydrophone," tech. rep., Defence Science and Technology Organisation, 2005.
- [29] O. Kilic *et al.*, "Miniature photonic-crystal hydrophone optimized for ocean acoustics," tech. rep., E. L. Ginzton Laboratory, Stanford University, 2011.
- [30] Progress Ultrasonic. (undated). Progress Ultrasonic Group. [Online]. Viewed 2014 February 5. Available: <http://www.progressultrasonicsgroup.com/pdf/>.
- [31] H. Wiacek, "Ultraschall - ein umweltfreundliches verfahren zur brunnenregenerierung," tech. rep., Institut der Johannes Gutenberg-Universität Mainz, 2004.